NATIONAL ADVISORY COMMITTEE FOR AERONAUTICS

TECHNICAL NOTE 3061

STRESSES AROUND RECTANGULAR CUTOUTS IN TORSION BOXES

By Paul Kuhn and James P. Peterson

Langley Aeronautical Laboratory
Langley Field, Va.

Washington
December 1953

NATIONAL ADVISORY COMMITTEE FOR AERONAUTICS

TECHNICAL NOTE 3061

STRESSES AROUND RECTANGULAR CUTOUTS IN TORSION BOXES

By Paul Kuhn and James P. Peterson

SUMMARY

A method is presented for calculating the stresses produced by rectangular cutouts of any size in torsion boxes. The problem is divided into a "box problem" and a "cover problem." The box problem is a special case of the general method of analyzing torsion boxes without cutouts. In the cover problem, simple shear-lag theory is used to obtain "key" stresses; the final distributions are obtained from these key stresses by means of simple rules or empirical distribution curves. Comparisons with the results from three series of tests in which the dimensions of the cutouts varied over a wide range are shown.

INTRODUCTION

The methods of calculating stresses around cutouts in aircraft shell structures are often based on rather arbitrary modifications of elementary theories. These methods have served reasonably well to predict the ultimate strength of structures made from highly ductile materials but they are often inadequate when less ductile materials are used and they are generally inadequate for fatigue calculations.

The general problem of calculating stresses around cutouts must be broken down into specific ones if reasonably simple solutions are to be obtained. One specific problem of great practical interest is that of determining the stresses around a rectangular cutout in the cover of a torsion box. Reference 1 presents a method of analysis which is very simple but which breaks down when the cutout becomes large. Reference 2 presents a method of analyzing a box with large cutouts; however, for the cover adjacent to the cutout, this method gives only chordwise averages of the shear flow and is thus not sufficiently complete.

In reference 3, the results of reference 2 are used and more detailed distributions of the stresses around the cutout are obtained by an analytical and a numerical method. The calculating procedures involved in using these methods were considered somewhat lengthy in view of the fact

that the accuracy achieved was not entirely satisfactory in the critical region near the cutout; moreover, the methods are rather inflexible in the sense that the computational labor is not reduced greatly if the problem posed is to find only the peak stress or the stresses at a few points.

In this paper, a unified method is presented which is applicable to cutouts of any size, provided only that coaming stringers are used. The analysis of the torsion-box action is made on the basis of the same assumptions as were made in reference 2, but the details of procedure have been changed in order to integrate the method with that of analyzing torsion boxes without cutouts as given in reference 4. A more detailed analysis of the cover containing the cutout is then made by utilizing an idealized structure and simple shear-lag theory to obtain "key" stresses. Finally, the complete distributions are obtained from the key stresses with the aid of empirical distribution curves or simple rules. Compared with the methods of reference 3, the present method requires considerably less labor, is more flexible, and gives better accuracy.

SYMBOLS

A	cross-sectional area of member carrying direct stress (when used without subscript signifies effective area of corner flange of an idealized four-flange torsion box of rectangular section), sq in.
A^*_{CSG}	area of coaming stringer in idealized panel at large distance from cutout, sq in. (see formula (3))
E	Young's modulus, ksi
F	force in stringer designated by subscript (if used without subscript, signifies force in coaming stringer at coaming rib), kips
G	shear modulus, ksi
I	moment of inertia, in.^{4}
K	shear-lag parameter, in.$^{-1}$
T	torque, in.-kips
V	transverse shear force in one side of net section, kips

X	force characterizing bicouple in a four-flange box, kips
a	length of bay, in.
b	width of rectangular box, in.
c	width of net section (one side), in.
d	half-length of cutout, in.
f	stress-distribution coefficient
h	depth of rectangular box, in.
p, q	unit warps associated with calculation of bending stresses due to torsion, in./kip
q	shear flow, kips/in.
q_p	shear flow in plane panel, kips/in. (fig. 2)
$(\overline{q})^F$	total shear flow on coaming stringer caused by force F, kips/in.
t	thickness, in.
t_x	equivalent thickness of sheet-stringer combination for normal stress, in.
w	half-width of cutout, in.
w_e	effective width used in conjunction with figure 7 (see formula (14) and fig. 8(a))
w^T	warp caused by torque, in.
x	spanwise coordinate within a bay measured inward from a bulkhead, in. (see fig. 1)
y	chordwise coordinate measured from the spanwise center line of a symmetrical box, in. (see fig. 3(b))
y_e	coordinate used in conjunction with figure 7 (equals y if $w < c$; defined in fig. 8(a) for $w > c$)
$\overline{y}$	distance from corner flange to neutral axis of net section, in.
ξ	spanwise coordinate measured from coaming rib (see fig. 3(b)), in.

σ	normal stress, ksi
τ	shear stress, ksi

Subscripts:

CF	corner flange
CO	cutout region between coaming ribs
COB	cutout bay
CS	coaming stringer
CSG	coaming stringer in gross section
CSN	coaming stringer in net section
F	flange (also used to denote front)
FG	edge or corner flange in gross section
FN	edge or corner flange in net section
N	net section
R	rear
b	pertains to horizontal wall of rectangular box
c	pertains to extended net section
e	effective
eq	equivalent
h	pertains to vertical wall of rectangular box
mod	modified
n	pertains to nth bay or station
w	pertains to wake panel

Superscripts:

F	caused by force in coaming stringer at coaming rib
T	caused by torque

Abbreviations:

N.A. neutral axis

C.S. coaming stringer

DEFINITION OF PROBLEM AND OUTLINE OF METHOD

The problem treated herein is that of finding the stresses around a rectangular cutout in a torsion box of the type shown schematically in figure 1. The figure also indicates the notations used, which are adopted from references 4 and 5.

The problem is solved to obtain approximate results in two steps. The first step is a torsion-box analysis of the type discussed in references 4 and 5, in which the elementary shear stresses due to torsion and the additional stresses that result from the tendency of each bay to restrain the warping of the adjacent bays are evaluated. In the second step, the cover is assumed to be detached from the box and is analyzed in more detail, with the local effects produced by the cutout in the adjacent full cover being calculated. The two parts of the problem are referred to as the "box problem" and the "cover problem." For small cutouts, the box effect is often negligible and only the cover problem needs to be solved. For this reason, and because the method for solving the box problem is only an extension of a previously published method, the cover problem is discussed first.

THE COVER PROBLEM

Definition of problem.- Figure 2 shows a stiffened panel representing the cover detached from the box and loaded by shear flows acting along the edges. The cover problem is to find the stresses in such a panel.

In order to obtain sufficient generality, the shear flow is assumed to have the value q_p' in the outer panels and the value q_p in the inner panel as indicated in figure 2. Each coaming rib is thus loaded by a shear flow q_p' on its outer edge and a flow q_p on its inner edge. The difference between q_p' and q_p is normally furnished by a load distributed along the length of the coaming rib; in figure 2, this load is shown for convenience as a concentrated force at the top of the rib.

The lower sketch in figure 2 indicates the deformation of the panel under load. The net section of the panel behaves evidently as a beam

restrained at the two ends. All references to beam action, bending, neutral axis, moment of inertia, and so forth in the following discussions refer to the bending of the net section in its own plane as depicted in figure 2.

The solution of the cover problem is based on the analysis of a highly simplified skeleton structure. For application to actual structures, some of the analytical formulas are modified empirically. The modified formulas yield key stresses in the actual structure. The complete distribution of the stresses is approximated by utilizing these key stresses and rules based on elementary theory or empirical coefficients.

The skeleton structure.- Figure 3(a) shows schematically the actual panel structure. For the derivation of the formulas, the following restrictive assumptions are made:

(a) The panel is flat and symmetrical about the longitudinal, as well as the transverse, center line.

(b) Stringers are of constant cross-sectional area.

(c) Sheet thicknesses are constant in each subpanel (defined by fig. 3(b)).

(d) The panel is very long, so that the disturbance produced by the cutout is negligibly small at the ends of the panel.

In addition, the standard assumption of simple shear-lag theory is made that the panel behaves as though it contained a system of closely spaced rigid transverse ribs.

Figure 3(b) shows the skeleton structure used. The cross-sectional areas of the skeleton stringers are obtained by the following procedures.

For the half net section of the actual structure, compute the moment of inertia I and the location $\bar{y}$ of the neutral axis N.A. which is measured as indicated in figure 3(a). The areas A_{CSN} and A_{FN} are determined by the condition that the skeleton net section must have the same moment of inertia and the same neutral axis as the actual net section. These requirements are fulfilled if the areas are calculated from the formulas

$$A_{CSN} = \frac{I}{c(c - \bar{y})} \tag{1}$$

$$A_{FN} = \frac{I}{c\bar{y}} \tag{2}$$

For the gross section, the skeleton areas are given by the expressions

$$A^{*}_{CSG} = A_{CSN} + \frac{1}{3} wt_x \tag{3}$$

$$A_{FG} = A_{FN} \tag{4}$$

The quantity t_x is the "stringer sheet" thickness of the material lying between the two coaming stringers in the actual structure (total cross-sectional area of stringers and effective sheet divided by total width $2w$). The quantity $\frac{1}{3} wt_x$ is equivalent to the quantity $\frac{1}{6} ht$ which is used in standard plate-girder theory to express the contribution of the web of the plate girder to the effective flange area. The asterisk signifies that the value of the area given by formula (3) is a limiting value which can be considered as valid only at a large distance from the cutout. This formula is sufficiently accurate to be used for calculating the shear-lag parameter K (formula 5); for the calculation of the stringer stresses, however, it will be replaced later by a more accurate value which varies along the span.

Figure 3(b) shows the coordinates used. The coordinate ξ (distance from coaming rib) is used in the calculation of stresses produced by the cutout, that is, in the numerical solution of the cover problem. The coordinate x is the standard one used in the solution of box problems as indicated in figure 1.

Figure 3(c) shows one-half of the skeleton structure (to the right of the transverse center line) exploded into free bodies. The analysis of the net-section part requires only simple statics; the forces V and F and the shear flow q_N are evidently

$$V = q_p \frac{b}{2} \tag{A}$$

$$F = q_p \frac{bd}{2c} \tag{B}$$

$$q_N = q_p \frac{b}{2c} \tag{C}$$

The system of forces acting on the gross section, shown on the right in figure 3(c), may be resolved into two sets. The first set consists of shears acting on the edges that produce simply a uniform shear flow q'_p

in the entire panel. The second set consists of the two couples formed by the forces F acting on the coaming stringers and the forces $F\frac{2w}{b}$ acting on the edge flanges as shown in figure 3(d). This set is self-equilibrated and is termed a "planar bicouple." The solution of the cover problem is thus reduced to the solution of the problem indicated by figure 3(d).

The internal forces produced in the gross section by the planar bicouple can be calculated by simple shear-lag theory. By analogy with the fundamental shear-lag problems for infinitely long panels, expressions for these forces may be written down as follows:

$$F_{CSG} = Fe^{-K\xi} \tag{D}$$

$$F_{FG} = F\frac{2w}{b}e^{-K\xi} \tag{E}$$

Then, by statics,

$$q_w^F = \frac{2c}{b}(\bar{q})^F \tag{F}$$

$$q_c^F = -\frac{2w}{b}(\bar{q})^F \tag{G}$$

where the quantity

$$(\bar{q})^F = FKe^{-K\xi} \tag{H}$$

has been introduced for convenience.

In the equations given, shear flows are considered positive if they act in the same sense as the shear flow q_p. Forces in the flanges and coaming stringers are considered positive if they act in the direction of the arrows shown in figure 3(d).

With the aid of these expressions and the principle of least work, the shear-lag parameter K is found to be defined by the expression

$$K^2 = \frac{\frac{G}{E}\left[\frac{1}{A^*_{CSG}} + \frac{1}{A_{FG}}\left(\frac{2w}{b}\right)^2\right]}{\frac{w}{t_w}\left(\frac{2c}{b}\right)^2 + \frac{c}{t_c}\left(\frac{2w}{b}\right)^2} \tag{5}$$

For $t_w = t_c = t$ this expression simplifies to

$$K^2 = \frac{Gt}{E}\left[\frac{1}{A^*_{CSG}} + \frac{1}{A_{FG}}\left(\frac{2w}{b}\right)^2\right]\left(\frac{1}{c} + \frac{1}{w}\right) \tag{5a}$$

The formulas just given represent the theoretical solution for the skeleton structure. For the analysis of actual structures, some of these formulas are modified empirically. In order to avoid confusion, the formulas carrying capital letters A to H are never referred to in actual analysis; only numbered formulas are used.

Key stresses in actual structure.- The stresses in the skeleton structure are intended to represent approximations to the most important or key stresses in the actual structure as follows:

(a) The stresses in the skeleton coaming stringers and edge flanges represent the stresses in the actual coaming stringers and edge flanges, respectively.

(b) The shear flow in the "wake panel" (between the coaming stringers) of the skeleton structure at any given station represents the chordwise average of the shear flow in the corresponding location of the actual structure. The same relation holds for the panel between coaming stringer and edge flange (net section and extended net section).

Tests have shown that the skeleton stresses interpreted in this manner give adequate accuracy, in general, for the net section and for the gross section in regions away from the cutout. The accuracy of the stresses is inadequate, however, for the gross section in the region close to the cutout. That the stresses may be inaccurate for this section was already implied in the discussion of expression (3). The term $\frac{1}{3} wt_x$ in this expression is based on the assumption that the chordwise distribution of the stresses in the cut stringers is linear, as shown in figure 4 by the solid line. This assumption holds reasonably well at large distances from the cutout. At moderate distances, however, the true distribution becomes S-shaped as indicated by the dashed line and, at very small distances, takes the extreme S-shape indicated by the long and short dashed line. In the skeleton structure this change in distribution is disregarded, and as a result the stringer stresses, as well as the shear stresses, are misrepresented to some extent in the vicinity of the cutout.

The formulas for the key stresses given in this section are based on the theoretical formulas for the skeleton structure. In order to

achieve adequate accuracy of stress prediction in the vicinity of the cutout, however, empirical modifications have been made to some of the formulas; comparisons with the lettered formulas presented in the preceding section indicate these modifications.

In these formulas, a positive sign for a normal stress signifies a tensile stress. The upper signs in formulas (7) and (8) apply when y is positive. For formulas (11) and (12), the signs are determined by the sign of the stress in the adjacent part of the net section.

Net section,

$$F = q_p \frac{bd}{2c} \tag{6}$$

$$\sigma_{CSN} = \pm \frac{F}{A_{CSN}} \left(\frac{x}{d} - 1 \right) \tag{7}$$

$$\sigma_{FN} = \mp \frac{F}{A_{FN}} \frac{2w}{b} \left(\frac{x}{d} - 1 \right) \tag{8}$$

$$q_N = q_p \frac{b}{2c} \tag{9}$$

Gross section,

$$A_{CSG} = A_{CSN} + \frac{1}{3} wt_x \left(1 - e^{-K\xi} \right) \qquad (w > c) \tag{10a}$$

$$A_{CSG} = A_{CSN} + \frac{1}{3} wt_x \left(1 - e^{-\frac{\xi}{w}} \right) \qquad (w < c) \tag{10b}$$

$$\sigma_{CSG} = \pm \frac{F}{A_{CSG}} e^{-K\xi} \tag{11}$$

$$\sigma_{FG} = \mp \frac{F}{A_{FG}} \frac{2w}{b} e^{-K\xi} \tag{12}$$

$$(\bar{q})^F = FKe^{-K\xi}\left(1 - \frac{1}{2}e^{-K\xi}\right) \qquad (w > c) \qquad (13a)$$

$$(\bar{q})^F = FKe^{-K\xi}\left(1 - \frac{2w}{b}e^{-\frac{\xi}{w}}\right) \qquad (w < c) \qquad (13b)$$

$$w_e = c + (w - c)\frac{2\xi}{w} \qquad \left(w > c;\ \xi < \frac{w}{2}\right) \qquad (14a)$$

$$w_e = w \qquad \text{(all other cases)} \qquad (14b)$$

$$b_e = 2(w_e + c) \qquad (15)$$

$$q_w^F = \frac{2c}{b_e}(\bar{q})^F \qquad (16)$$

$$q_c^F = -\frac{2w_e}{b_e}(\bar{q})^F \qquad (17)$$

$$q_w = q_p' + q_w^F \qquad (18)$$

$$q_c = q_p' + q_c^F \qquad (19)$$

The empirical modification terms in formulas (10) and (13) contain the parameter K when $w > c$ and the parameter $1/w$ when $w < c$. This change in parameters does not imply a serious discontinuity because $K \approx \frac{1}{w}$ when $w = c$ for reasonably conventional configurations.

Distribution of stresses in actual structure.- The normal stresses in the net section may be separated into those arising from the bending moment produced by the transverse force V and those produced by the edge shear q_p. The solid lines in figure 5(a) show the distribution of the normal stress due to V as calculated by the elementary theory of bending; the curve of chordwise distribution is a straight line passing through the neutral axis. The dashed lines indicate qualitatively expected deviations from the simple theory caused by local shear lag.

Figure 5(b) shows the stringer stresses caused by the edge shears. The chordwise distribution shown - a straight line beginning at the neutral axis - is arbitrarily assumed.

Superposition of the two types of stringer stresses for a given station results in figure 5(c), which expresses pictorially the rule by which the stringer stresses in the net section can be estimated from the key stresses σ_{CSN} and σ_{FN}.

Figure 5(d) shows the chordwise distribution of the shear stresses in the net section as expected from qualitative considerations of shear lag. In the central portion ($x \approx d$), the distribution follows closely the elementary VQ/It formula. Near the root, shear lag may cause a radical redistribution, with the result that the maximum stress may be found next to the coaming stringer rather than at the neutral axis.

Tests show that the shear-lag effects vary greatly and that other effects may cause further changes in the distribution. On the basis of tests, the distribution shown in figure 5(e) is suggested for purposes of ultimate-strength design. If fatigue is a design consideration, some allowance should be made for the stress peak shown in figure 5(d) at the corner of the cutout.

The stringer stresses in the gross section may be estimated from the key stresses at a given station by use of the straight-line diagram shown in figure 4. Attempts to refine the distribution for the wake panel by using S-shaped distribution curves near the cutout are probably not worthwhile because the stringers in this region are very unlikely to be critical in design.

For the shear flows, the reverse is true; that is, the shear flows in the wake panel near the cutout are critical in design. The maximum value of the shear flow caused by the forces F occurs at the rib station; the shear flow always adds numerically to the basic shear flow q'_p (for a panel such as the one shown in fig. 3(a)). As a result, it is also necessary to estimate the chordwise distribution.

Such an estimate may be made with the aid of curves of distribution coefficients drawn on the basis of test results. Figure 6 shows schematically a family of chordwise curves of the distribution coefficients f for a half-width cutout plotted in isometric projection in order to give a picture of the entire distribution. In the wake panel, the distribution at the rib station follows a parabola. With increasing distance from the cutout, the curve flattens out and finally becomes an upside-down parabola. The area under the curve remains constant along the span; the mean height of the curve is unity. The final shear flow at any given point in the wake panel is obtained by multiplying the

distribution coefficient f by the shear flow q_w^F, given by formula (16), which represents the chordwise average between coaming stringers. In the extended net section (panel between a coaming stringer and the adjacent edge flange), the shear flow q_c^F, given by formula (17), is distributed in a similar manner; the chordwise distribution for this panel is taken as uniform at the rib station and changes rather quickly to a half-parabola (see fig. 6).

The shape of the distribution curves is a function of the distance ξ. If the curves are to be general, this function must be nondimensional. Tests indicate that the function may be taken as $K\xi$ for $w > c$ and as ξ/w for $w < c$.

The curves are based on tests of panels that had heavy edge flanges; whereas, the coaming stringers were of the same size as the regular stringers. If the coaming stringer is very heavy compared with the other stringers at the distance $K\xi = 1.5$ and beyond, a better approximation will probably be obtained by assuming that the distribution in the wake panel is uniform at $K\xi = 1.5$ and that the distribution in the extended net section is uniform along the span.

Figure 7 gives curves from which the distribution coefficients may be read for the wake panel.

The solid curves correspond to the distribution shown in figure 6; the dashed curves give the suggested distribution for the case where the coaming stringers are heavy at $K\xi = 1.5$ and beyond. In general, stations for analysis will be dictated by considerations of rib locations. The spanwise curves of distribution coefficients (fig. 7(a)) can then be used to obtain five coefficients for any given station, which should be sufficient to construct the chordwise curves of shear flow; if necessary, guidance in this construction may be obtained by inspecting the chordwise curves in figure 7(b).

Curves of distribution coefficients for the net-section panel are not given because the suggested chordwise distributions follow simple laws except in the region between $K\xi = 0$ and $K\xi = 0.5$. The construction of curves for this region is not believed to be worthwhile because experimental distribution curves vary so much from case to case that the uniform distribution shown for $K\xi = 0$ can be rated only as a very rough approximation, too rough to justify any elaboration.

The distribution curves of figure 7 are directly applicable as noted only when the cutout is a half-width one ($2w = b/2$, or $w = c$). When the cutout is wider ($w > c$), the central portion of the wake panel carries almost no shear stress near the end. For the sake of simplicity, complete ineffectiveness is assumed for a V-shaped region as indicated

in figure 8(a); the remainder of the half-width of the wake panel is termed "effective width" and is defined by expression (14a). The distribution curve is applied to the effective width as though it were an actual width; that is, the coordinate y_e is measured from the edge of the V-notch as indicated in figure 8(a).

As the cutout becomes narrower than half-width, the distribution may be thought of as resulting from the overlapping of the two halves of the "basic" curve for the half-width cutout (fig. 8(b)), and the distribution approaches a uniform one as the cutout becomes very narrow. The simplest possible approximation for this range is to modify the distribution coefficients according to the expression

$$f_{mod} = 1 + (f - 1)\frac{4w}{b} \qquad (w < c) \qquad (20)$$

Simplifications of procedure.- Some of the procedures given may be simplified somewhat in order to reduce computation time.

The largest item in the preliminary work is the computation of the moment of inertia of the net section. This computation can be eliminated if the assumption is made that the neutral axis lies halfway between the coaming stringer and the corner flange. The area of the skeletonized coaming stringer is then given by the expression

$$A_{CSN} = A_{CS} + \frac{c}{6} t_x \qquad (21)$$

The approximation will be too rough if the net section is narrow and the corner flange is much heavier than the coaming stringers.

For very narrow cutouts (say, $w < 0.1 \times b$), the shear-lag parameter may be computed by the simplified formula

$$K^2 \approx \frac{Gt_w}{EwA^*_{CSG}} \qquad (22)$$

and the shear flows in the gross section may be computed by the simplified expressions

$$q_w^F = FKe^{-K\xi} \qquad (23)$$

$$q_c^F \approx 0 \qquad (24)$$

The distribution factor f should be taken as equal to unity in such cases.

Comparison of expressions (22) and (5a) shows that the simplified expression will yield a somewhat lower value of K; the resulting effect on the peak value of the shear flow q_w tends to be counteracted by the omission of the term in parentheses from expression (13b) which results in expression (23).

The stress in the coaming stringer in the gross section may be taken as

$$\sigma_{CSG} = \frac{F}{A_{CSN}} e^{-K\xi} \tag{25}$$

unless the coaming stringer is heavily reinforced in the region of the net section, as by a doorframe.

For cutouts that are wide ($w > c$) and short ($2d < b$), it is suggested that the value q_N be used for the entire net section instead of using the more elaborate distribution obtained by the VQ/I formula because poor agreement between calculation and tests renders the elaboration useless (see section entitled "Experimental Evidence").

Comparison with previous method.- Since the simplifications of procedures given in the preceding section result in a set of formulas which resembles the set given in reference 1, a comparison of the relative merits of the two methods may be made.

In the liquidating-force method of reference 1 the stresses in the panel are considered as arising from the superposition of two loading cases (fig. 9). Case A produces simply a uniform shear flow in the entire panel; case B is solved approximately with the aid of simplifying assumptions concerning the stresses produced by the reversed or liquidating shear flow $-q_p$.

The simplifying assumptions are as follows:

(a) The transverse liquidating shear flows set up forces confined to the coaming ribs (fig. 10(a)) and balanced by shear flows confined to the region between these ribs (the net section of the panel).

(b) The longitudinal liquidating forces set up forces confined to the coaming stringers (fig. 10(b)) and balanced by shear flows in the region between these stringers.

The simplifying assumption (b) is supplemented by the rule that the coaming stringer is assisted by one-half of the strip of skin lying between it and the adjacent stringer.

The assumption that only the coaming stringer carries longitudinal stress is equivalent to assuming that the shear lag in the net section is very large. The liquidating-force method thus makes an automatic and conservative allowance for the local stress peak indicated in figure 5(a), whereas the method of this paper does not.

Another advantage of the liquidating-force method is that calculation of the cutout effects does not require a knowledge of the structure away from the cutout. A minimum requirement of the present method is that the width c of the net section be known; if the cross section of the torsion box is not simple, defining c may be difficult or impossible (for instance, in a multicell torsion tube).

Unfortunately, these potentially important advantages of the liquidating-force method are offset by an important disadvantage: namely, that the method must be regarded as unreliable except in special cases. Critical examination of the data in reference 1 shows that the rule concerning the effective width of skin assisting the coaming stringer is very important because the skin contributes a very substantial portion of the total effective area. Consider now the following hypothetical experiments.

Assume that the actual stringers, except the coaming stringer, are replaced by a large number of equally spaced small stringers having the same total area. The actual stress in the coaming stringer would now be expected to be less than in the original test case because some stringer material is now close to the coaming stringer, in a location where it will carry some stress. The calculated stress in the coaming stringer, on the other hand, would be much higher because there is now practically no effective width of skin as defined by the rule given. Similarly, if the original stringers are combined into a smaller number of larger stringers, the rule results in a much larger change of stress than would be expected from physical reasoning and the change is again in the opposite direction.

The hypothetical experiments show that any rule that defines the effective width of skin in terms of the stringer pitch cannot be considered to have general validity. The good agreement between test and calculation shown in reference 1 can therefore be expected only in the following special cases:

(a) cases in which the configuration of the cross section is similar to that of the test specimens of reference 1

(b) cases in which the coaming stringer is so heavy that the effective width of skin furnishes only an unimportant contribution.

THE BOX PROBLEM

General method.- The general method used herein for solving the box problem is that given in reference 4. For the sake of simplicity, the discussion in this section is confined to boxes having rectangular doubly symmetrical cross sections. Stations and bays of the box are numbered as in figure 1.

The stresses in bay n are caused by two sets of loads (fig. 11): namely, a torque T acting on each end face, and a self-balanced group of four forces X (a bicouple) acting on the four flanges at each end. The statically redundant bicouples X are computed for the entire box by solving a set of equations written with the aid of the recurrence formula (ref. 4)

$$q_n X_{n-1} - (p_n + p_{n+1})X_n + q_{n+1}X_{n+1} = -w_n^T + w_{n+1}^T \tag{26}$$

The quantities p and q express the warp of the cross section of a given bay at the near and the far end, respectively, caused by a bicouple of unit magnitude acting at the near end. The quantity w^T is the warp caused by the torque. Further discussion of details such as boundary conditions may be found in reference 4.

After the bicouples X have been computed, the stresses caused in any given bay by the bicouples acting on the two ends of the bay can be computed and added to the stresses caused directly by the torque.

Full bay.- For a full bay (without cutout), the procedure of reference 4 calls for replacing an actual cross section such as shown in figure 12(a) by an idealized or skeleton section as shown in figure 12(b). On the basis of the standard assumption that the normal stresses vary linearly in the chordwise direction (fig. 12(c)), the area A of the skeleton flange is computed by the formula

$$A = A_{CF} + \frac{1}{6} bt_x + \frac{1}{6} ht_h \tag{27}$$

where

A_{CF} area of corner flange proper

t_x stringer-sheet thickness of cover

The warps needed for use with equation (26) are given by the expressions

$$pG = \frac{aG}{3AE} + \frac{1}{8a}\left(\frac{b}{t_b} + \frac{h}{t_h}\right) \tag{28}$$

$$qG = -\frac{aG}{6AE} + \frac{1}{8a}\left(\frac{b}{t_b} + \frac{h}{t_h}\right) \tag{29}$$

$$w^T G = \frac{T}{8bh}\left(\frac{b}{t_b} - \frac{h}{t_h}\right) \tag{30}$$

Expressions (28) to (30) give the warps multiplied by the shear modulus G. These modified warps are more convenient to calculate than the unmodified values of p, q, and w^T because they do not contain the individual moduli G and E; only the ratio G/E is needed.

The shear flows in the walls of bay n are given by the expressions

$$q_b = \frac{T}{2bh} - \frac{X_n - X_{n-1}}{2a} \tag{31}$$

$$q_h = \frac{T}{2bh} + \frac{X_n - X_{n-1}}{2a} \tag{32}$$

These shear flows are considered to apply to the idealized, as well as to the actual, cross section.

The normal stress in the corner flange (idealized or actual) varies linearly from the value X_{n-1}/A at station n - 1 to X_n/A at station n. The normal stresses in the actual stringers can be deduced from the flange stresses at any given station by the straight-line relation indicated in figure 12(c). The signs of these stresses are determined by inspection with the aid of figure 11 which shows positive bicouples.

Qualitative considerations of cutout bay.- In reference 2, a method was presented for solving what is termed here the box problem for a special case: namely, a box which consisted of a bay containing a full-length

cutout and lying between two full bays and which was loaded by torques at the two ends. The set of tests reported in this reference showed that the physical assumptions made yielded a rather satisfactory solution. The method given herein is therefore based on the same assumptions; the presentation is changed, however, in order to obtain a procedure which makes it possible to treat a cutout bay in the same manner as a full bay, that is, as part of a long torsion box.

The bay containing the cutout is skeletonized as indicated in figure 13(a). When the bay forms part of a torsion box, bending deformation of the coaming ribs in the plane of the cover is prevented by the adjacent full cover. For the isolated bay, the coaming ribs are therefore assumed stiff against bending; this assumption is indicated pictorially in figure 13(a) by showing the ribs as heavy bars. With stiff coaming ribs, the two parts of the top cover can act as two beams "in parallel," built-in at both ends and undergoing bending deflection, as well as shear deflection, within their plane; the bay can then act in essentially the same manner as a full bay and can carry torques as well as bicouples.

Figure 13(b) shows the longitudinal forces that exist at the juncture between an idealized cutout bay and the adjacent full bay. The coaming rib and the bulkhead, which are common to both bays, are shown separated from the bays. On the side toward the cutout bay, the rib is loaded by two couples formed by the forces in the coaming stringers and those in the corner flanges, respectively. On the side toward the full bay, the rib is loaded by only one couple formed by the forces in the corner flanges. The assumption that the coaming rib is stiff thus separates the box problem from the cover problem. A remark on this assumption is made in the section entitled "Limitations of Method."

Formulas for cutout bay.- The idealized cross section of a cutout bay is shown in figure 14. The area A_F is obtained in the same manner as for a full bay by formula (27). The areas A_{CSN} and A_{FN} are calculated by expressions (1) and (2) with one difference in detail (which is generally unimportant): namely, that the effective area $\frac{1}{6} ht_h$ should be added to the area of the corner flange proper before the moment of inertia I of the net section is computed.

Figure 15 shows free-body diagrams of the individual parts of the cutout bay. Application of the equilibrium equations, aided by these diagrams, yields the following expressions if the cutout bay is the nth bay of the box:

Torque loading,

$$q_b = q_h = \frac{T}{2bh} \qquad q_N = \frac{T}{4ch} \tag{33}$$

$$F_{CSN} = \pm\frac{Ta}{8hc}\left(\frac{2x}{a} - 1\right) \tag{34}$$

$$F_{FN} = \mp\frac{Taw}{4bch}\left(\frac{2x}{a} - 1\right) \tag{35}$$

$$F_F = 0$$

Bicouple loading,

$$q_b = -\frac{X_n - X_{n-1}}{2a} \tag{36}$$

$$q_h = \frac{X_n - X_{n-1}}{2a} \tag{37}$$

$$q_N = q_b \frac{b}{2c} \tag{38}$$

$$F_{CSN} = \mp X_{n-1} \frac{b}{4c}\left(1 - \frac{x}{a}\right) \mp X_n \frac{b}{4c} \frac{x}{a} \tag{39}$$

$$F_{FN} = \pm\frac{1}{2} X_{n-1}\left(1 + \frac{b}{2c}\right)\left(1 - \frac{x}{a}\right) \pm \frac{1}{2} X_n\left(1 + \frac{b}{2c}\right)\frac{x}{a} \tag{40}$$

$$F_F = X_{n-1}\left(1 - \frac{x}{a}\right) + X_n \frac{x}{a} \tag{41}$$

The upper signs in formulas (34), (35), (39), and (40) apply when y is positive; a positive force signifies a tensile stress. The sign of the stress caused by the force F_F (formula (41)) is determined by inspection from figure 11.

Expressions (33) to (41), used in conjunction with the method of dummy loading (ref. 4), yield the following expressions for warps:

$$pG = \frac{aG}{6E}\left[\frac{1}{A_F} + \frac{b^2}{16c^2A_{CSN}} + \frac{1}{4A_{FN}}\left(1 + \frac{b}{2c}\right)^2\right] + \frac{1}{16a}\left(\frac{b}{t_b} + \frac{b^2}{2ct_N} + \frac{2h}{t_h}\right) \quad (42)$$

$$w^TG = \frac{T}{16bh}\left(\frac{b}{t_b} + \frac{b^2}{2ct_N} - \frac{2h}{t_h}\right) + \frac{1}{384}\frac{G}{E}\frac{Ta^2b}{hc^2A_{CSN}} + \frac{1}{384}\frac{G}{E}\frac{Ta^2(b^2 - 4c^2)}{bhc^2A_{FN}} \quad (43)$$

The expression for qG is similar to that for pG, except that the first (bracket) term is multiplied by $-\frac{1}{2}$. The expressions for pG, qG, and w^TG reduce to those for a full bay (expressions (28) to (30)) when $w = 0$ and A_{CSN} is infinite.

THE COMPLETE PROBLEM

General procedure.- The general procedure for solving the complete problem involves the following steps:

(1) Each bay is skeletonized (formulas (27) and (1) to (3); see first paragraph of section entitled "Formulas for cutout bay").

(2) The warps are calculated (formulas (28) to (30), (42), and (43)).

(3) A system of equations is set up with the aid of the recurrence formula (26) and is solved to find the bicouples X.

(4) The shear flows due to box action are found by formulas (31) and (32) for the full bays. The calculation of the associated stringer stresses is discussed in the paragraph following formula (32).

(5) Shear flows for the cutout bay are found by formulas (33) and (36) to (38). Key stringer stresses for the cutout bay are found by formulas (34), (35), (39), and (40).

(6) The total shear flow q_N from formulas (33) and (38) is distributed according to the scheme of figure 5(e) if desired. Stringer stresses in the net section are deduced from the key stresses according to the scheme of figure 5(c).

(7) The force F is computed by formulas (34) and (39) as F_{CSN} for $x = 0$ and $x = a$.

(8) The cover problem as defined by figure 3(d) is solved. Key stresses are calculated by formulas (10) to (17). The shear stresses are distributed with the aid of the coefficients given in figure 7; the stringer stresses, if needed, are deduced from the key stresses according to the scheme of figure 4.

(9) The distributed stresses obtained in step (8) are added to the cover stresses obtained in step (4) for the bays affected by the cutout.

In the procedure just given, the analysis of the net section is part of the solution of the box problem, not part of the solution of the cover problem if the latter is visualized in the form shown in figure 2. Concomitantly, formulas (6) to (8), (18), and (19) do not appear in the procedure. The reason for not using the analysis based on figures 2, 3(a), and 3(c) is that these figures define the specialized case in which the loading is symmetrical about the transverse center line of the cutout. The procedure given applies to the general case when this symmetry does not exist. Figure 3(c) could be modified to apply to the general case, but the procedure used was judged to be somewhat more convenient.

Complications.- In practice, various complications of the problem are encountered.

The box problem is complicated by deviations of the actual cross section from the rectangular doubly symmetrical configuration. For cross sections such as suggested by figure 1, adequate accuracy is obtained if a rectangular section having the same average depth is substituted. The procedure is indicated by the numerical example given in the appendix.

An important complication may arise from the configuration of the coaming stringer. The area of this stringer is often increased in the region of the cutout in order to compensate for the material eliminated by the cutout; in the full section, the area is tapered off. For such cases, the following procedure is suggested on the basis of a procedure developed and verified experimentally for simple shear-lag problems:

(a) Compute a preliminary value of the shear-lag parameter K by formulas (5) and (3). Find the area of the coaming stringer proper at station $K\xi = 0.5$ and use it instead of the area of the coaming stringer in the cutout region to repeat the calculations with formulas (1) to (5). Use the new value of K for further calculations. A third computation cycle for K should be made if the variation of area is extreme.

(b) Add to the expression for A_{CSG} in equations (10a) or (10b) the term $-\Delta A$ signifying the amount by which the area of the coaming

stringer proper at a given station is decreased below the value at the rib station ($\xi = 0$). Use these local values of A_{CSG} for computing the stresses by formula (11).

Another complication may be that the length 2d of the cutout is less than the length a of the bay; the formulas given for cutout bays are then not applicable. This complication usually arises only when the cutout is not very wide; this fact permits the use of a simple approximate procedure which is also useful in other cases. This procedure consists in replacing the cover containing a cutout by a cover containing no cutout and of such thickness that the shear deformations as defined by the displacements of the four corners are the same for the original and the replacement cover. In order to find the thickness of this cover, assume first that only the cutout region of length 2d between the two coaming ribs is to be replaced by a solid cover. By the application of elementary formulas to the deformation of the net section (fig. 2), the thickness of this solid cover is found to be defined by the expression

$$\left(\frac{1}{t_b}\right)_{CO} \approx \frac{b}{2ct_N} + \frac{d^2bG}{6EI} \tag{44}$$

The thickness of a uniform solid cover extending over the entire length a of the cutout bay (COB) is then defined by the expression

$$\left(\frac{1}{t_b}\right)_{COB} = \left(\frac{1}{t_b}\right)_{CO} \frac{2d}{a} + \frac{a - 2d}{at_b} \tag{45}$$

where t_b denotes the thickness of the original cover in the region between coaming rib and end of bay.

Now, let t_{b2} denote the thickness of the cover opposite the cutout one. The equivalent average defined by the expression

$$\left(\frac{1}{t_b}\right)_{eq} = \frac{1}{2}\left[\left(\frac{1}{t_b}\right)_{COB} + \frac{1}{t_{b2}}\right] \tag{46}$$

is then used in place of t_b in formulas (28) to (30) to compute the warps.

These formulas may, of course, also be used for a bay with a full-length cutout in order to avoid the use of the rather cumbersome formulas (42) and (43). Note, however, that expression (44) is approximate

and becomes of questionable accuracy when the bending term becomes much larger than the shear term. The accuracy is probably adequate in most cases for cutouts up to half-width.

Limitations of method.- Qualitative theoretical considerations and a study of the test results (presented subsequently) indicate some limitations of the method.

If the cutout is small (narrow as well as short), the net section constitutes a short but deep beam which does not follow the elementary theory of bending very well as a result of shear lag. The effect of such proportions on the shear in the net section is believed to be taken care of fairly well by the distribution scheme shown in figure 5(e). The effect on the stress in the coaming stringer can be taken care of by a small arbitrary allowance. A definitely conservative estimate of this stress can be obtained by assuming that the area A_{CSN} is equal to the area of the actual coaming stringer alone.

If the cutout is wide ($w > c$) and short ($2d < b$), tests show that the total transverse shear force in the net section is less than calculated and that the distribution may differ markedly from the calculated one. The difference in total shear force is believed to result from the fact that the corner flange carries more than its share of the shear; such action has been found in other cases and indicates that a built-up beam may not follow the elementary theory of bending closely. The inadequacy of the theory results in conservative predictions of shear and stringer stresses in the net section but unconservative predictions for the corner flanges, which suffer secondary bending.

The assumption that the warping characteristics of a full bay are not affected by the presence of a cutout in the adjacent bay becomes questionable when the full bay is short. Tests indicate satisfactory agreement in cases where the length of the full bay was equal to one-half the width of the box. Bulkheads are unlikely to be spaced at closer intervals; ribs may be, but present practice tends toward wider spacing. If the question appears to be important, one or two steps of a successive-approximation procedure might be used in which the standard formulas for the unit warps are corrected for the stress disturbance produced by the adjacent cutout.

EXPERIMENTAL EVIDENCE

The experimental evidence presented here is obtained from three sets of tests, two of which have been published previously.

Test Series I

Test specimens and general discussion.- The first set of tests, reported originally in reference 1, was made on the box shown in figure 16. The loading torque was introduced through the two bosses on the end bulkhead, and the reacting torque was applied in the same manner; consequently, there was no restraint against warping at the ends of the box which would introduce undesired stresses. The cover containing the cutout was riveted to the side walls and the end bulkheads of the box but not to the intermediate bulkheads in an attempt to suppress box action and thus to produce the conditions of a pure cover problem. In order to check whether this aim had been achieved, the following calculations were made.

On the assumption that the cover was riveted to the bulkheads, the equivalent thickness was computed by expression (46) for all tests. For the two tests showing the smallest equivalent thickness (and consequently the largest box effect), the box effect was computed. In the most extreme case (test 12), the cover shear was changed by about 33 percent. The measured stresses, however, agreed very closely with the calculations based on the assumption of no box effect; the conclusion was, therefore, that the device of not riveting the cover to the intermediate bulkheads had achieved the aim of reducing box effect to a negligible amount. For the next case, the box effect was of the same order of magnitude as the estimated experimental error; for all other cases, it was much less. Thus, box effect could have been neglected in all but two cases even if the cover had been riveted to all bulkheads. All calculations shown are therefore made without accounting for box effect.

The original test schedule is shown in table I. The original test numbers shown in this table have been retained in order to avoid confusion, but in the figures, the tests have been rearranged to give a logical sequence.

The plots for the first 3 tests (three smallest cutouts) have been omitted here because they are not particularly informative, the stress disturbance being small. The agreement between test and calculation for these tests varies from good to fair.

Shear stresses.- The shear stresses for tests 4 to 12 are shown in figures 17 to 21. For the wake panel (between the coaming stringers), the agreement between measured and calculated stresses is very satisfactory, except perhaps for a tendency to underestimate somewhat the stresses along the line $y = 0$ in the longer cutouts (tests 10, 11, and 12).

In the extended net section (portion of gross section lying between coaming stringer and corner flange), the calculated chordwise distribution is based on the curves shown in figure 6. Previously mentioned is

the fact that the uniform distribution assumed for station $K\xi = 0$ can be rated only as a rough approximation because the actual distributions can vary considerably in this vicinity. For the tests of series I, however, the agreement is generally rather satisfactory except for test 6 (fig. 18(b)) where the experimental stresses in panel 2 (sheet panel next to the coaming stringer) are higher than the calculated stresses. The excess stress in this panel is more or less balanced by deficiencies in sheet panels 1 and 6. It should be noted that the cutout in test 6 is the longest one in the entire series and that the gross section is not long enough to let the disturbance decay to a negligible value at the end of the box as is assumed in the theory.

For the net section, the calculated distribution is based on the diagram shown in figure 5(e). The agreement is rather satisfactory for this set of tests as long as the width of the cutout is less than one-third of the width of the box (figs. 17 to 19). For a width equal to one-half the width of the box or more (figs. 20 and 21), the agreement varies from poor to very poor. The calculated distribution curves may differ from the measured ones rather markedly at times. Moreover, all the measured shear stresses at a given station are lower than the calculated stresses in many cases. The latter discrepancies can be explained qualitatively by the assumption that the heavy corner angle carries a larger part of the shear than application of the VQ/I formula to the net section would indicate. The existence of such load transfer from shear web to heavy angle in the vicinity of discontinuities has been proved in cases where the total shear force was either known (on plate girders) or could be measured to a rather high degree of accuracy (on torque boxes in which shear measurements were made around the entire perimeter). For the tests under consideration herein (figs. 20 and 21), the stress predictions are highly conservative for the skin. The presence of a variable shear in the corner angles, however, connotes secondary bending stresses in these angles which may be very important.

Stringer stresses.- The stringer stresses for tests 4 to 12 are shown in figures 22 to 26. Inspection of the stresses in the coaming stringers shows rather good agreement between tests and calculations except for a region about 2 inches to either side of the coaming rib. In this region, the experimental curves show either a local peak (figs. 22 and 23) or a local dip (figs. 24 to 26). A local peak may be expected as a result of local shear lag and is indicated schematically in figure 5(a). A local dip may result from two causes. The first is a difference between nominal and actual geometry. For purposes of calculation, the length of the cutout is measured between the two lines of rivets connecting the sheet to the coaming ribs. The sheet, however, actually extends about 1 inch inside these lines; the effective area of the coaming stringer is thus less than the assumed area. The second cause is the stiffening effect exerted by the coaming rib on the adjacent sheet. All three effects would be smaller in practice than in these tests because the coaming stringers would be reinforced.

The stresses in the other stringers are estimated fairly well by the calculations except for short cutouts, where they are overestimated. These discrepancies are not felt to be serious for practical design problems.

Test Series II

Test specimens and general discussion.- The tests of series II were made on the box shown in figure 27 and were first reported in reference 2. Data on test conditions are given in table II. As in the tests of series I, no restraint against warping existed at the ends of the box.

The box was originally not built for the cutout tests; for the original purpose, it was considered adequate to make all but the end bulkheads "floating" on top of the stringers (see sketch in lower right-hand corner of fig. 27). For the first four cutout tests, the torque-transfer bulkheads at the ends of the cutout were made "semifloating" (directly connected to top skin). For the last test, these bulkheads were connected to top and bottom skin (see sketch in upper left-hand corner).

A semifloating bulkhead must be regarded as having a finite (and small) stiffness in shear; the shear stiffness was determined in reference 2 by special tests (the equivalent thickness, obtained from ref. 2, is given in table II). The procedure for taking this finite shear stiffness into account is given in reference 5. The calculations on box effect were taken directly from reference 2 which gave a specialized method, applicable to the test box, based on the same assumptions as the method of the present paper.

In two of the tests of series II, tests 3 and 4, the cutout was the same; the only difference was that the two bulkheads lying in the cutout region were removed for test 4. The full-floating intermediate bulkheads shown in figure 27 were disregarded in all computations because their shear stiffness is very low and because these bulkheads would not change the stress conditions significantly even if they were very stiff.

Results.- Measured and calculated shear stresses are shown in figures 28 to 31. The station numbers signify distances in inches from the center line of the cutout. The results for tests 3 and 4 are shown in one figure (fig. 30, for the torque used in test 4) because the only physical change made in the box (removal of the two bulkheads in the cutout region) does not affect the calculations, and the differences in measured stresses were negligible.

The agreement between test and calculation is most satisfactory except for two items. One is the distribution of the stresses in the

net section in the root region close to the end of the cutout. These tests are the main ones responsible for the statement made previously that the uniform distribution for the end zone shown in figure 5(e) can be rated only as a rough approximation because the true distribution is often more nearly as indicated in figure 5(d). In test 1 (fig. 28), a large discrepancy in the total shear occurs at station $24\frac{1}{2}$, comparable to the discrepancies found in the net sections of the four tests in series I with the widest cutouts. On the other hand, the stresses in the central portions of the net sections agree well with the calculations for tests 1 and 2 (fig. 29) of series II in spite of the fact that the cutouts are much wider than those in the tests of series I.

The experimental stresses in tests 3 and 4 (fig. 30) also show unsatisfactory agreement with the calculations. The distribution of the cover shears at stations $32\frac{1}{2}$ and $37\frac{1}{2}$ shows rather poor agreement, and the total web shears at stations $22\frac{1}{2}$ and $27\frac{1}{2}$ show very poor agreement. Two main reasons are apparent why the theory might be expected to become unreliable for these tests.

When the net section is narrow, the shear distribution is governed essentially by the action of the panel formed by the coaming stringer, the corner flange, and the connecting sheet. A glance at the net section in figure 27 shows that a very large disparity exists in size and shape between the stringer and the corner angle. Moreover, the width of the panel is very ill defined. The width is about 2 inches if measured between the rivet line on the coaming stringer and the inner rivet line on the corner angle. However, since there is some shear deformation between inner and outer rivet line, the width should be measured to some undefinable line between these two rivet lines; the resulting uncertainty is large because the total width is so small.

The second source of error arises from the very low shear stiffness of the bulkheads. With such a large cutout, each bulkhead is obviously expected to transfer a large couple from the shear webs to the cover, and the theory assumes that this transfer is effected by the bulkhead itself. Because the bulkhead is so flexible, however, the box walls in its vicinity tend to act as distributed frame ribs which effect a portion of the transfer. This action takes place in any box but is quantitatively negligible with bulkheads of normal shear stiffness.

In test 5 (fig. 31), the agreement is again rather satisfactory for the cover shears as well as the web shears. This observation suggests that the main reason for the disagreements in tests 3 and 4 is the use of very flexible bulkheads on a very large cutout.

Of some concern are the shear measurements on the bottom cover in the cutout bay in the last three tests with a wide cutout. The curves at stations 0, $12\frac{1}{2}$, and $22\frac{1}{2}$ show high local peaks near the corner flange. Similar peaks have sometimes been noted in other tests on torsion boxes with discontinuities and suggest that some margin of safety should be provided in such regions.

The agreement between the calculated and experimental stresses in the coaming stringers and flanges (fig. 32) is rather satisfactory, particularly in view of the extreme narrowness of the net section in the last three tests, a condition which brings about an appreciable uncertainty in the location of the true neutral axis for the built-up cross section with its large disparity in size between compression flange and tension flange.

Test Series III

Test specimens.- The two tests of series III were made on the box shown in figure 33. In the first test, the cutout was as shown in the figure. In the second test, the cutout was widened by one sheet panel on each side (four stringers cut instead of two). At the root end of the box, warping was fully restrained because the box was symmetrical about the plane of the root.

Results.- Measured and calculated shear stresses are shown in figures 34 and 35. Station numbers signify distances from the tip in inches. The calculations were made under certain simplifying assumptions as discussed in the appendix, where the calculations for test 2 are given in some detail as a numerical example. At the stations close to the end of the cutout, the calculations overestimate the shear stresses near the center line ($y = 0$), contrary to the tendency noted in the tests of series II. These discrepancies are of no practical interest because the stresses here are at a relative minimum. At the same stations, there is not entirely satisfactory agreement in the region between coaming stringer and flange. Outside of these discrepancies, however, the agreement is satisfactory. The experimental plots show dissymmetries which may be attributed to the fact that the cross section is trapezoidal.

The stresses in the coaming stringers are shown in figures 36 and 37. The agreement is excellent except for the local dips below the calculated peaks for two of the curves.

CONCLUDING REMARKS

This paper presents a method for calculating stresses around rectangular cutouts in torsion boxes. Also presented are the results of three series of tests in which the dimensions of the cutouts vary over a wide range.

The comparisons between calculated and experimental stresses may be summed up broadly by stating that the agreement is satisfactory on the whole with the following exceptions:

(a) When the cutout is narrow and short, the calculation underestimates the peak stresses in the coaming stringers because no allowance is made for shear lag.

(b) When the cutout is wide and short, the calculation overestimates the transverse shear force in the net section, and the distribution also shows poor agreement. The discrepancies tend to decrease as the length of the cutout increases and appear to be negligible when this length exceeds the width of the box.

In case (a), the method is unconservative. However, the stress disturbance set up by a cutout small in both directions is not severe and covers only a small area. No undue weight penalty will therefore be incurred if an arbitrary conservative allowance is made in design.

In case (b), the method gives conservative predictions for the stresses in the skin. The degree of conservativeness is probably exaggerated by the tests because the coaming stringers would be heavier in practice than they were in the tests. A certain degree of conservativeness is felt to be desirable in this case because the region in question is very likely to be critical in design. Attention is called to the fact that the differences between tests and calculations imply the existence of secondary bending in the spar caps; this aspect of the problem has not been investigated.

Langley Aeronautical Laboratory,
National Advisory Committee for Aeronautics,
Langley Field, Va., September 25, 1953.

APPENDIX

NUMERICAL EXAMPLE

As a numerical example, the last test presented in the section entitled "Experimental Evidence" (test 2 of series III) has been chosen; this example includes the complication of analyzing a nonrectangular section. In these calculations the ratio G/E is taken as 0.377. The torque is 73.5 inch-kips.

Idealization of full bays for box problem.- The cross section of the box is shown in figure 33(a). An approximately equivalent rectangular section 9 inches deep is used in the calculations. The approximation is somewhat rough because the ratio of depth of front spar to depth of rear spar is rather large, but it is sufficiently accurate for obtaining the stresses around the cutout, which is the main item of concern.

Moment of inertia of the front spar . . . . . 42.9 $in.^4$
Moment of inertia of the rear spar . . . . . 5.10 $in.^4$

An average moment of inertia is calculated by the expression

$$\frac{1}{I_{av}} = \frac{1}{2}\left(\frac{1}{42.9} + \frac{1}{5.10}\right) = \frac{1}{9.10}$$

which gives an equivalent concentrated flange area of

$$\frac{2(9.10)}{81} = 0.225 \text{ sq in.}$$

for a spar 9 inches deep.

Area of cover skin	33.0(0.040)	= 1.320 sq in.
Area of stringers	8(0.090)	= 0.720 sq in.
	bt_x	= 2.040 sq in.
	$1/6bt_x$	= 0.340 sq in.

The area of the corner flange of the idealized rectangular box 9 inches deep is

$$A = 0.225 + 0.340 = 0.565 \text{ sq in.}$$

The ratios b/t_b and h/t_h are

$$\frac{b}{t_b} = \frac{33.0}{0.040} = 825$$

$$\frac{h}{t_h} = \frac{1}{2}\left(\frac{12}{0.102} + \frac{6}{0.051}\right) = 117.5$$

Warps for full bays.- By formulas (28) to (30), the warps for the full bays are

$$pG = \frac{15(0.377)}{3(0.565)} + \frac{1}{8(15)}(825 + 117.5) = 11.20$$

$$qG = -\frac{15(0.377)}{6(0.565)} + \frac{1}{8(15)}(825 + 117.5) = 6.19$$

$$w^TG = \frac{73.5}{8(33.0)9.0}(825 - 117.5) = 21.9$$

Idealization of cutout bay.- The cutout, which is 16 inches long ($2d = 16.0$ inches) and five panels wide ($2w = 20.0$ inches), is located centrally in the cutout bay. For the purpose of idealizing the cover of the cutout bay, the width is measured along the cover between the centroids of the corner angles and is $b = 34.02$ inches. The width of the net section is

$$2c = 34.02 - 20.0 = 14.02 \text{ in.}$$

The properties of the two net sections differ somewhat. This difference is taken into account in the calculation of stresses in the coaming stringers; for the calculation of shear flows, average values are used.

Moment of inertia of front net section	6.61 $in.^4$
Moment of inertia of rear net section	5.12 $in.^4$

The average moment of inertia is given by

$$\frac{1}{I_{av}} = \frac{1}{2}\left(\frac{1}{6.61} + \frac{1}{5.12}\right) = \frac{1}{5.76}$$

By formula (44),

$$\left(\frac{1}{t_b}\right)_{CO} = \frac{34.02}{14.02(0.040)} + \frac{64.0(34.02)(0.377)}{6(5.76)} = \frac{1}{0.0119}$$

by formula (45),

$$\left(\frac{1}{t_b}\right)_{COB} = \frac{1}{0.0119}\left(\frac{16.0}{30.0}\right) + \frac{1}{0.040}\left(\frac{14.0}{30.0}\right) = \frac{1}{0.0177}$$

and by formula (46),

$$\left(\frac{1}{t_b}\right)_{eq} = \frac{1}{2}\left(\frac{1}{0.0177} + \frac{1}{0.040}\right) = \frac{1}{0.0246}$$

Therefore,

$$\frac{b}{t_b} = \frac{33.0}{0.0246} = 1340$$

and, as calculated before,

$$\frac{h}{t_h} = 117.5$$

A concentrated corner area of 0.565 square inches is used as in the idealized full bay; this approximation is justified for the box problem by the fact that the material eliminated by the cutout is relatively inactive in carrying normal stresses.

By formulas (28) to (30), the warps for the cutout bay are

$$pG = \frac{30.0(0.377)}{3(0.565)} + \frac{1}{8(30.0)}(1340 + 117.5) = 12.75$$

$$qG = -\frac{30.0(0.377)}{6(0.565)} + \frac{1}{8(30.0)}(1340 + 117.5) = 2.73$$

$$w^{T}G = \frac{73.5}{8(33.0)9.0}(1340 - 117.5) = 37.8$$

Shear stresses due to box action.- With the warps for all the bays determined, the recurrence formula (formula (26)) yields the following set of equations

$$\begin{aligned}
-22.40X_1 + 6.19X_2 &= 0 \\
6.19X_1 - 22.40X_2 + 6.19X_3 &= 0 \\
6.19X_2 - 23.95X_3 + 2.73X_4 &= 15.9 \\
2.73X_3 - 23.95X_4 + 6.19X_5 &= -15.9 \\
6.19X_4 - 22.40X_5 + 6.19X_6 &= 0 \\
6.19X_5 - 11.20X_6 &= -21.9
\end{aligned}$$

The solution of these equations is

$$X_1 = -0.051 \text{ kips}$$

$$X_2 = -0.185 \text{ kips}$$

$$X_3 = -0.617 \text{ kips}$$

$$X_4 = 0.828 \text{ kips}$$

$$X_5 = 0.908 \text{ kips}$$

$$X_6 = 2.457 \text{ kips}$$

With these X-forces, the stresses due to box action can be computed for the entire box. In this example, detailed calculations are given for the shear stresses at station 62 (in the net section) and at the spanwise station $1\frac{1}{8}$ inches from either end of the cutout. Both of these stations are in the cutout bay. The shear flow in the bottom cover and in the gross section of the top cover is, by formulas (33) and (36),

$$q_b = \frac{73.5}{2(33.0)9.0} - \frac{0.828 + 0.617}{2(30.0)}$$

$$= 0.1238 - 0.0241 = 0.0997 \text{ kips/in.}$$

or

$$\tau_b = \frac{0.0997}{0.040} = 2.49 \text{ ksi}$$

The shear flow due to torque loading in the vertical walls is, by formula (33),

$$q_h = 0.1238 \text{ kips/in.}$$

The shear flows in the vertical walls due to the bicouple loading are

$$(q_h)_F = 0.0241\left(\frac{h_R}{h}\right)^2 = 0.0241\left(\frac{36}{81}\right) = 0.0107 \text{ kips/in.}$$

and

$$(q_h)_R = 0.0241\left(\frac{h_F}{h}\right)^2 = 0.0241\left(\frac{144}{81}\right) = 0.0428 \text{ kips/in.}$$

$$(\tau_h)_F = \frac{0.1238 + 0.0107}{0.102} = 1.32 \text{ ksi}$$

$$(\tau_h)_R = \frac{0.1238 + 0.0428}{0.051} = 3.27 \text{ ksi}$$

The factors $(h_R/h)^2$ and $(h_F/h)^2$ are obtained from the statics of a four-flange box of trapezoidal cross section.

The shear force in the net section is calculated by formulas (33) and (38) as

$$V = cq_N = \frac{73.5}{4(9.0)} - 0.0241\left(\frac{33.0}{2}\right) = 2.040 - 0.398 = 1.642 \text{ kips}$$

The stresses caused by this force are calculated by the elementary VQ/It formula and are shown plotted in figure 35 for station 62 which is 2 inches from the center line of the cutout.

Shear stresses due to planar bicouples F.- The average moment of inertia of the net section is $I = 5.76$ inches^4. An average value of $\bar{y}$ is 2.12 inches. Other pertinent dimensions are

$$c = 7.01 \text{ in.}$$

$$w = 10.0 \text{ in.}$$

$$b = 2(10.0 + 7.01) = 34.02 \text{ in.}$$

By formulas (1) and (3),

$$A^*_{CSG} = \frac{5.76}{7.01(7.01 - 2.12)} + \frac{1}{3}\,10\left(0.040 + \frac{0.090}{4}\right)$$

$$= 0.168 + 0.208 = 0.376 \text{ sq in.}$$

By formulas (2) and (4),

$$A_{FG} = \frac{5.76}{7.01(2.12)} = 0.388 \text{ sq in.}$$

By formula (5a),

$$K^2 = 0.377(0.040)\left[\frac{1}{0.376} + \frac{1}{0.388}\left(\frac{20.0}{34.02}\right)^2\right]\left(\frac{1}{7.01} + \frac{1}{10.0}\right)$$

$$= 0.0130$$

$$K = 0.114$$

The force F is calculated from the shear force V as

$$F = V\frac{d}{c} = \frac{1.642(8.0)}{7.01} = 1.873 \text{ kips}$$

For $\xi = 1.12$ inches, $K\xi = 0.128$ and $e^{-K\xi} = 0.880$.

By formula (14a),

$$w_e = 7.01 + (10.0 - 7.01)\frac{2(1.12)}{10} = 7.68 \text{ in.}$$

By formula (15),

$$b_e = 2(7.68 + 7.01) = 29.38 \text{ in.}$$

By formula (13a),

$$(\bar{q})^F = 1.873(0.114)(0.880)\left(1 - \frac{0.880}{2}\right) = 0.1050 \text{ kips/in.}$$

or

$$(\bar{\tau})^F = 2.62 \text{ ksi}$$

By formulas (16) and (17),

$$\tau_w^F = \frac{2(7.01)}{29.38}2.62 = 1.25 \text{ ksi}$$

$$\tau_c^F = -\frac{2(7.68)}{29.38}2.62 = -1.37 \text{ ksi}$$

These values of τ_w^F and τ_c^F are average values. The final shear stress in the cover is obtained by properly distributing τ_w^F and τ_c^F and adding the results to the shear stress calculated in the previous section (2.49 ksi).

The shear stress τ_w^F is distributed according to the distribution charts of figure 7(a) which give a distribution coefficient for $\frac{y_e}{w_e} = 0$, 0.25, 0.50, 0.75, and 1.00 where y_e is measured from a line which is $w - w_e = 10.00 - 7.68 = 2.32$ inches from the center line of the panel (see fig. 8(a)). Addition of $f\tau_w^F$ and the average shear stress (2.49 ksi) results in the final shear stresses as shown in the following table:

①	②	③	④	⑤
$\frac{y_e}{w_e}$	f	$f\tau_w^F$	τ_b (average)	③ + ④
0	0.03	0.037	2.49	2.527
.25	.28	.350	2.49	2.840
.50	.87	1.085	2.49	3.575
.75	1.70	2.120	2.49	4.610
1.00	2.42	3.020	2.49	5.510

The above values are plotted in figure 35 for station $50\frac{3}{4}$ $\left(\xi = 1\frac{1}{4} \text{ inches}\right)$ and station 69 (ξ = 1 inch). The calculations were made for $\xi = 1\frac{1}{8}$ inches.

The shear stresses in the extended net section are obtained in a similar manner. The distribution coefficients for this case were obtained by assuming a uniform distribution at $K\xi = 0$, a parabolic distribution at $K\xi = 0.5$, and a linear variation with $K\xi$ in the region between $K\xi = 0$ and $K\xi = 0.5$.

Coaming-stringer stresses.- In calculating the stresses in the coaming stringers, average values are used for F and K but individual values are used for calculating the area of the coaming stringer. These values are

$$F = 1.873 \text{ kips}$$

$$K = 0.114$$

For the net section near the front spar,

$$I = 6.61 \text{ in.}^4$$

$$\bar{y} = 1.81 \text{ in.}$$

$$c = 7.07 \text{ in.}$$

(c is measured between centroids of flange and coaming stringer angles.) By formulas (1) and (10a),

$$A_{CSN} = \frac{6.61}{7.07(7.07 - 1.81)} = 0.178 \text{ sq in.}$$

$$A_{CSG} = 0.178 + \frac{1}{3}(10.0)\left(0.040 + \frac{0.090}{4}\right)\left(1 - e^{-0.114\xi}\right)$$

$$= 0.178 + 0.208\left(1 - e^{-0.114\xi}\right)$$

and by formula (11),

$$\sigma_{CSG} = \frac{1.873e^{-0.114\xi}}{0.178 + 0.208\left(1 - e^{-0.114\xi}\right)}$$

For three values of ξ the evaluation of this formula gives

ξ	0.114ξ	$e^{-0.114\xi}$	σ_{CS}, ksi
0	0	1.000	10.50
2	.228	.797	6.78
4	.456	.635	4.69

The above values of stress are plotted in figure 37(a).

For the net section near the rear spar,

$$I = 5.12 \text{ in.}^4$$

$$\bar{y} = 2.42 \text{ in.}$$

$$c = 6.95 \text{ in.}$$

$$A_{CSN} = \frac{5.12}{6.95(6.95 - 2.42)} = 0.163 \text{ sq in.}$$

$$A_{CSG} = 0.163 + 0.208\left(1 - e^{-0.114\xi}\right)$$

$$\sigma_{CS} = \frac{1.873e^{-0.114\xi}}{0.163 + 0.208\left(1 - e^{-0.114\xi}\right)}$$

ξ	σ_{CS}, ksi
0	11.50
2	7.26
4	4.98

These values are plotted in figure 37(b).

REFERENCES

1. Moggio, Edwin M., and Brilmyer, Harold G.: A Method for Estimation of Maximum Stresses Around a Small Rectangular Cut-Out in a Sheet-Stringer Panel in Shear. NACA WR L-64, 1944. (Formerly NACA ARR I4D27.)

2. Kuhn, Paul, and Moggio, Edwin M.: Stresses Around Large Cut-Outs in Torsion Boxes. NACA TN 1066, 1946.

3. Rosecrans, Richard: A Method for Calculating Stresses in Torsion-Box Covers With Cutouts. NACA TN 2290, 1951.

4. Kuhn, Paul: A Method of Calculating Bending Stresses Due to Torsion. NACA WR L-352, 1942. (Formerly NACA ARR, Dec. 1942.)

5. Ebner, Hans: Torsional Stresses in Box Beams With Cross Sections Partially Restrained Against Warping. NACA TM 744, 1934.

TABLE I

BASIC DATA FOR TEST SPECIMENS OF SERIES I

Test	t, in.	d, in.	w, in.	T, in.-kips	$\frac{T}{2bht}$, ksi
1	0.0325	2	1.5	135	3.83
2	.0325	2	4.5	135	3.83
3	.0325	2	7.5	90	2.55
4	.0352	7	1.5	135	3.54
5	.0352	14	1.5	108	2.83
6	.0352	21	1.5	108	2.83
7	.0348	7	4.5	117	3.11
8	.0348	7	7.5	117	3.11
9	.0348	7	10.5	90	2.39
10	.0318	13	4.5	90	2.61
11	.0318	13	7.5	63	1.83
12	.0318	13	10.5	54	1.56

TABLE II

BASIC DATA FOR TEST SPECIMENS OF SERIES II

Test	t, in.	t_B, in.	d, in.	w, in.	T, in.-kips	$\frac{T}{2bht}$, ksi
1	0.063	0.00194	24.5	14.6	99.75	1.540
2	.063	.00194	24.5	19.1	92.70	1.432
3	.063	.00194	24.5	23.6	71.30	1.100
4	.063	.00194	24.5	23.6	64.12	.991
5	.063	.375	26.0	23.6	64.12	.991

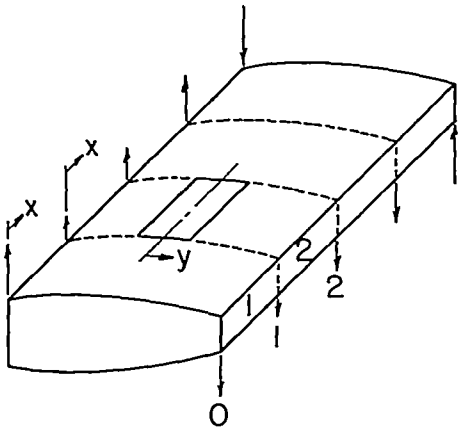

Figure 1.- Torsion box with cutout.

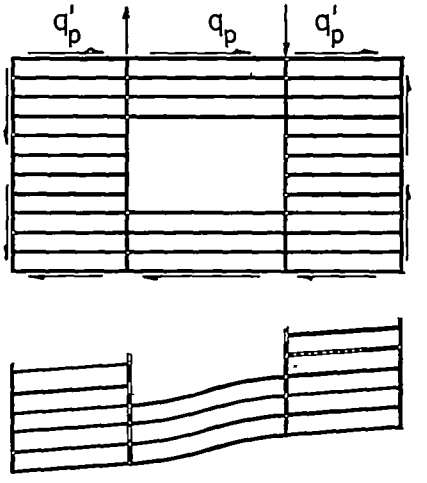

Figure 2.- Deformation of panel with cutout.

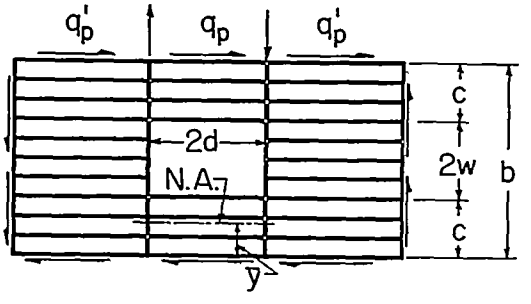

(a) Actual panel.

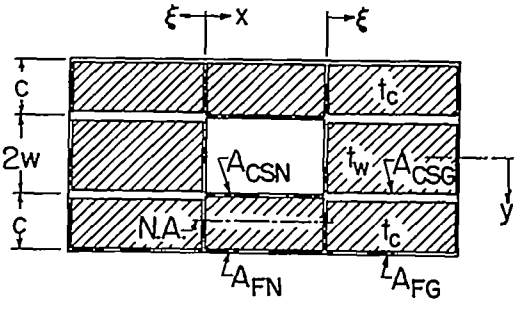

(b) Skeleton panel.

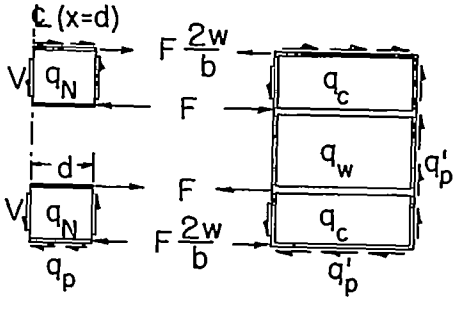

(c) Skeleton panel exploded.

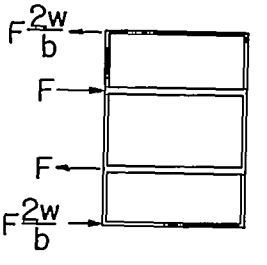

(d) Final problem.

Figure 3.- Simplification of cutout panel.

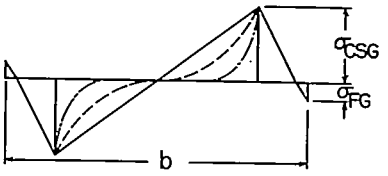

Figure 4.- Normal-stress distribution in gross section.

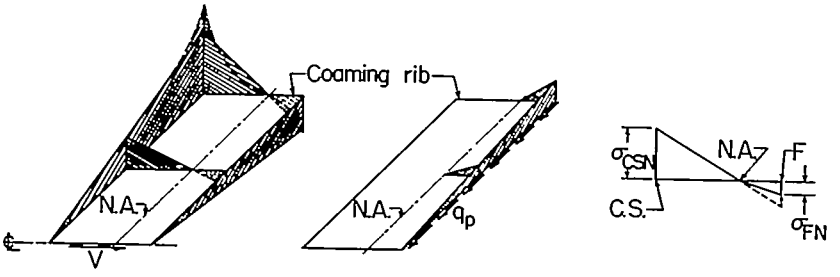

(a) Normal stress due to V.

(b) Normal stress due to q_p.

(c) Total normal stress.

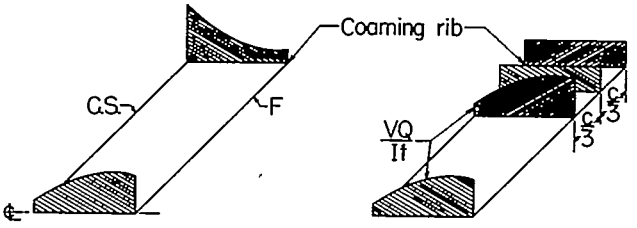

(d) Actual shear stress.

(e) Assumed shear stress.

Figure 5.- Stress distribution in net section.

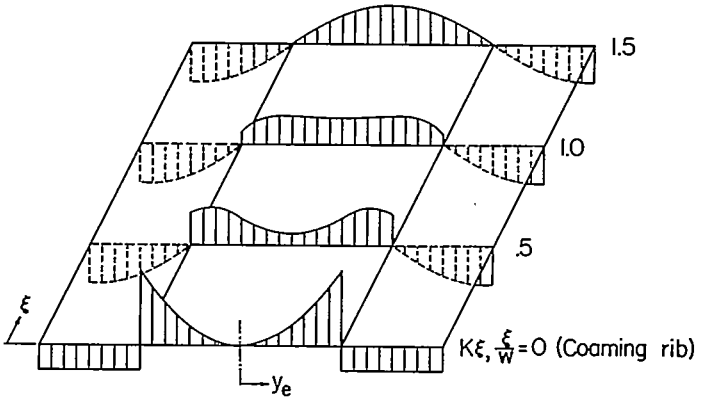

Figure 6.- Shear-stress-distribution coefficients for half-width cutout. (Shown schematically.)

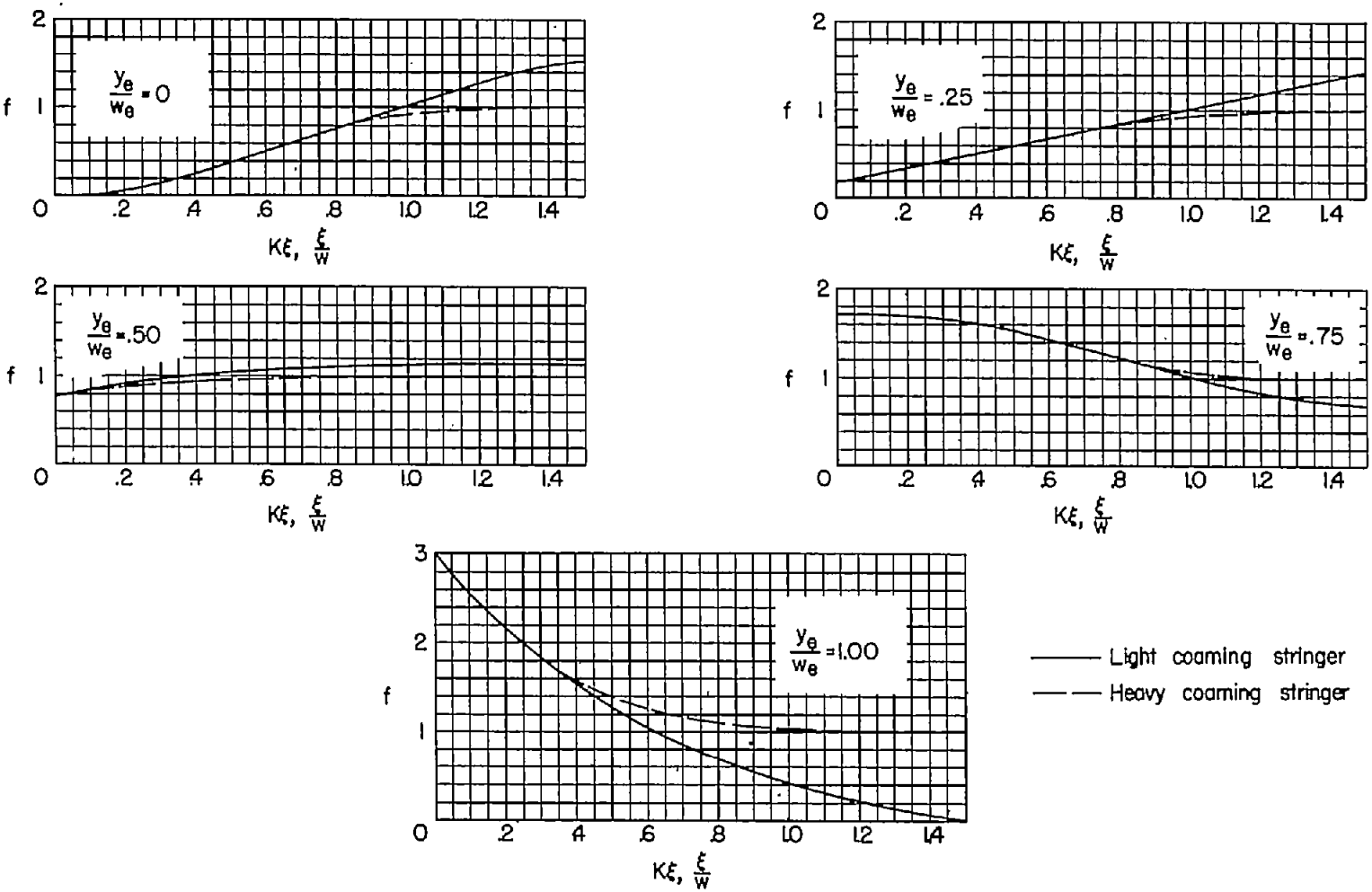

(a) Spanwise plots.

Figure 7.- Shear-stress-distribution coefficients. (For $w > c$, use $K\xi$; for $w < c$, use ξ/w.)

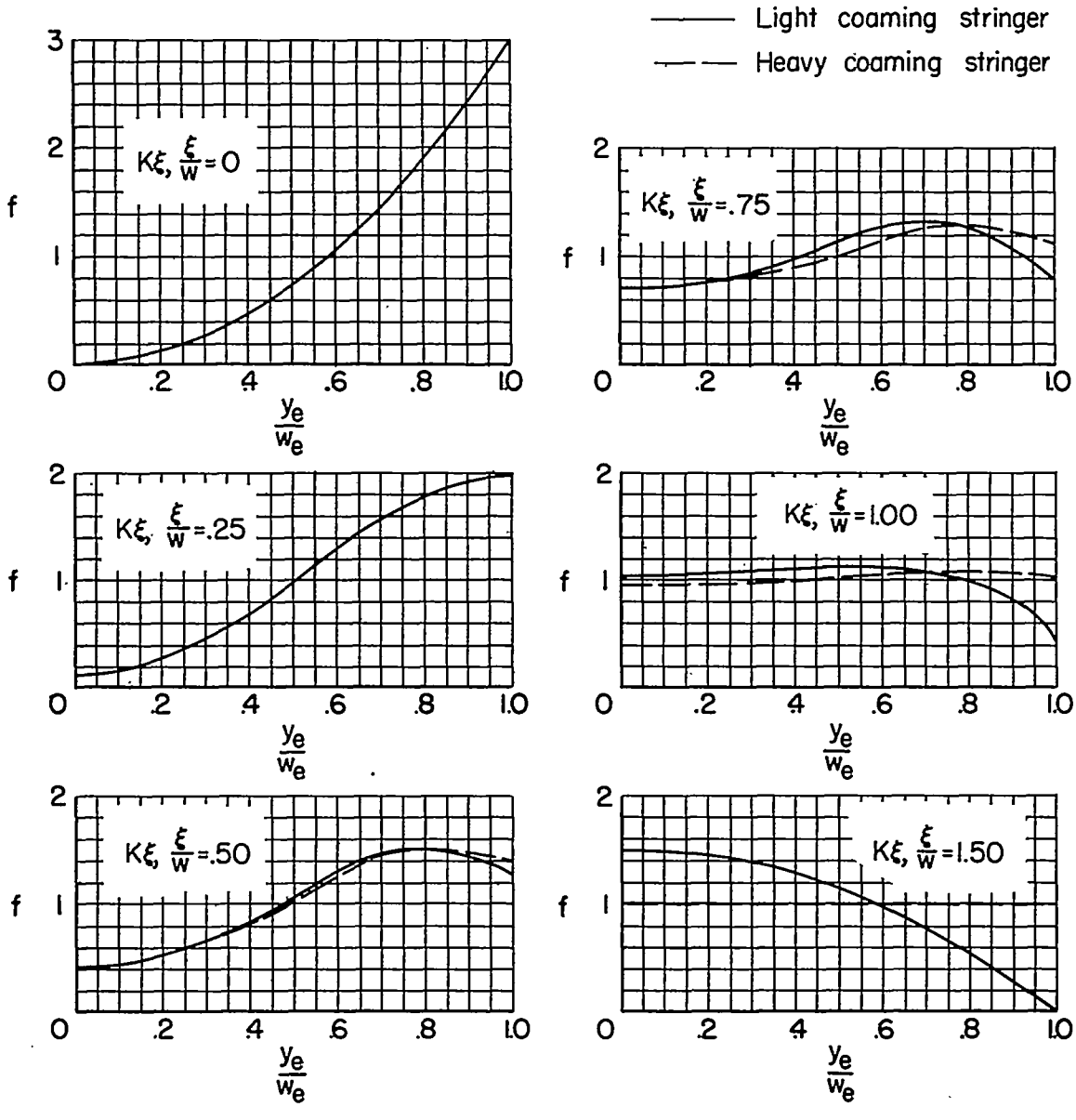

(b) Chordwise plots.

Figure 7.- Concluded.

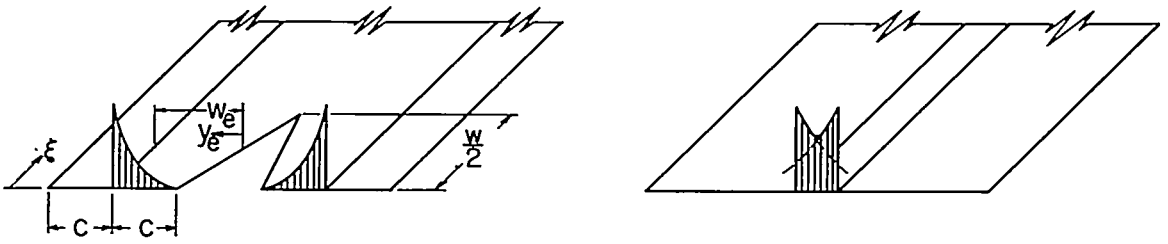

(a) Wide cutout. (b) Narrow cutout.

Figure 8.- Modification to shear-stress distribution for cutouts which are not half-width.

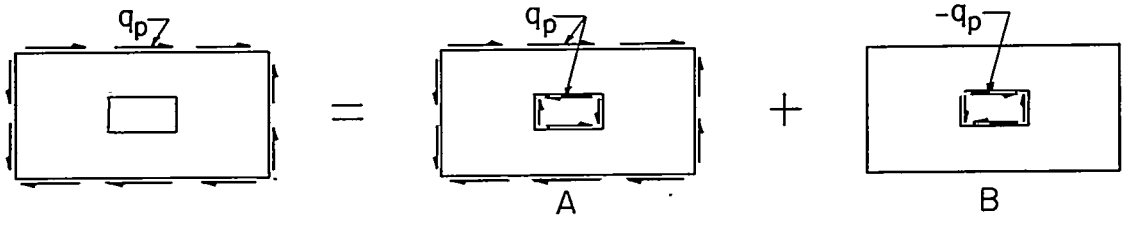

Figure 9.- Liquidating-force concept.

(a) Coaming-rib stress. (b) Coaming-stringer stress.

Figure 10.- Normal stresses in coaming members.

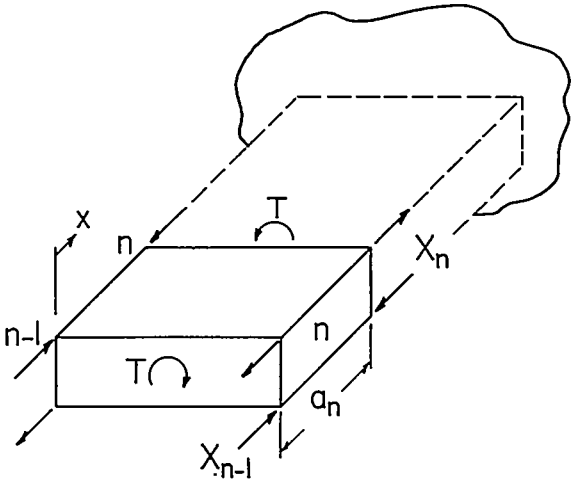

Figure 11.- Notation for box problems.

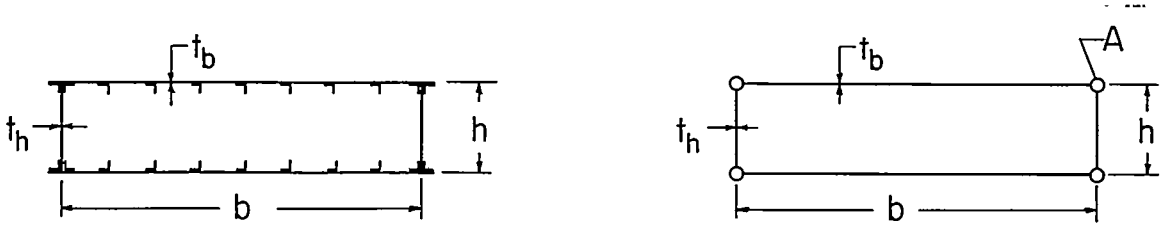

(a) Actual cross section.

(b) Idealized cross section.

(c) Normal-stress distribution.

Figure 12.- Idealization of cross section of torsion box.

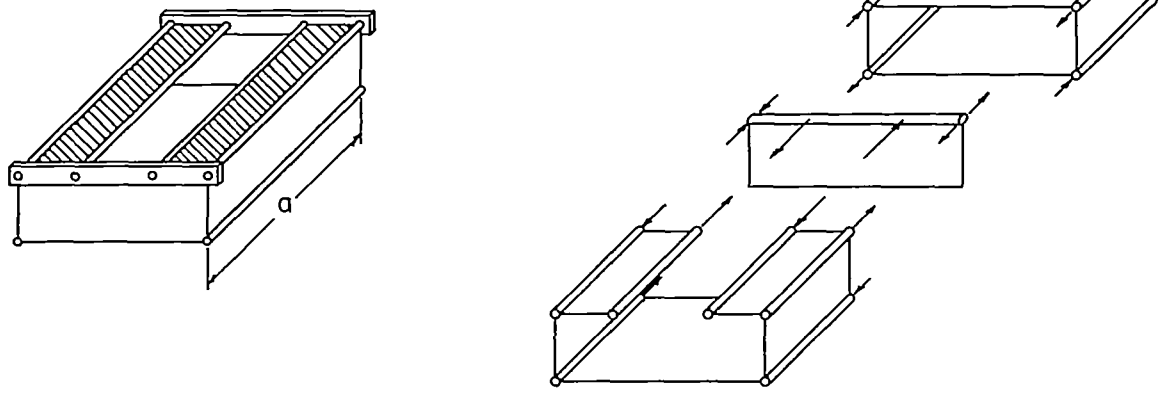

(a) Cutout bay as individual structure.

(b) Exploded view showing axial forces.

Figure 13.- Cutout bay.

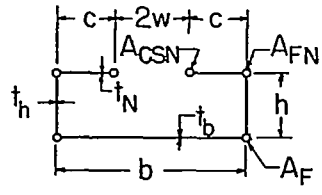

Figure 14.- Idealized cross section of cutout bay.

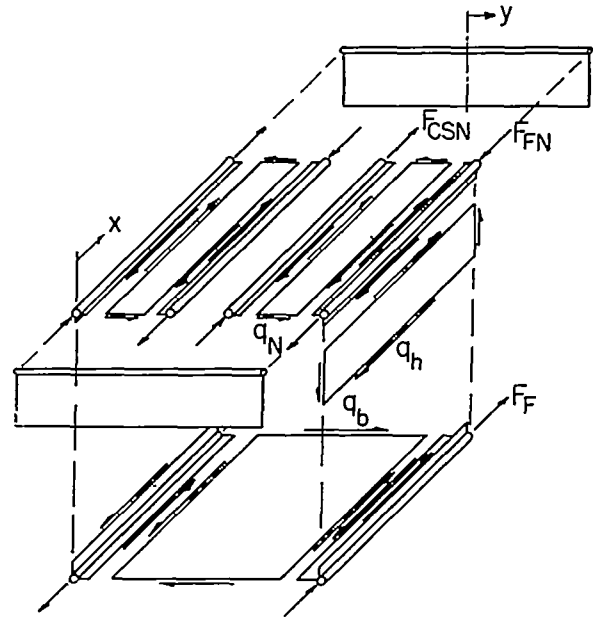

Figure 15.- Exploded view of cutout bay.

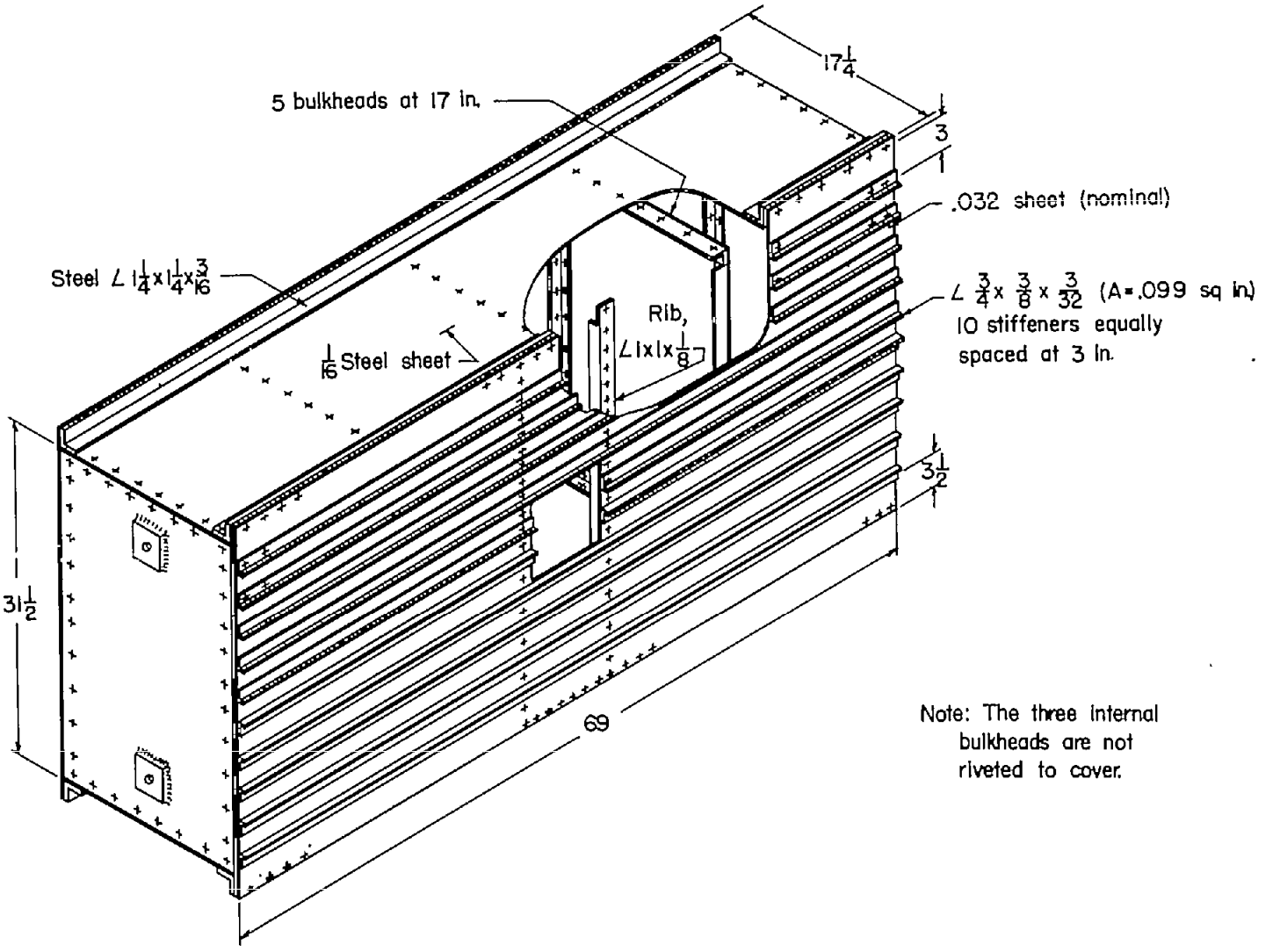

Figure 16.- Test box for series I tests. (All material 24S-T aluminum alloy except where noted.)

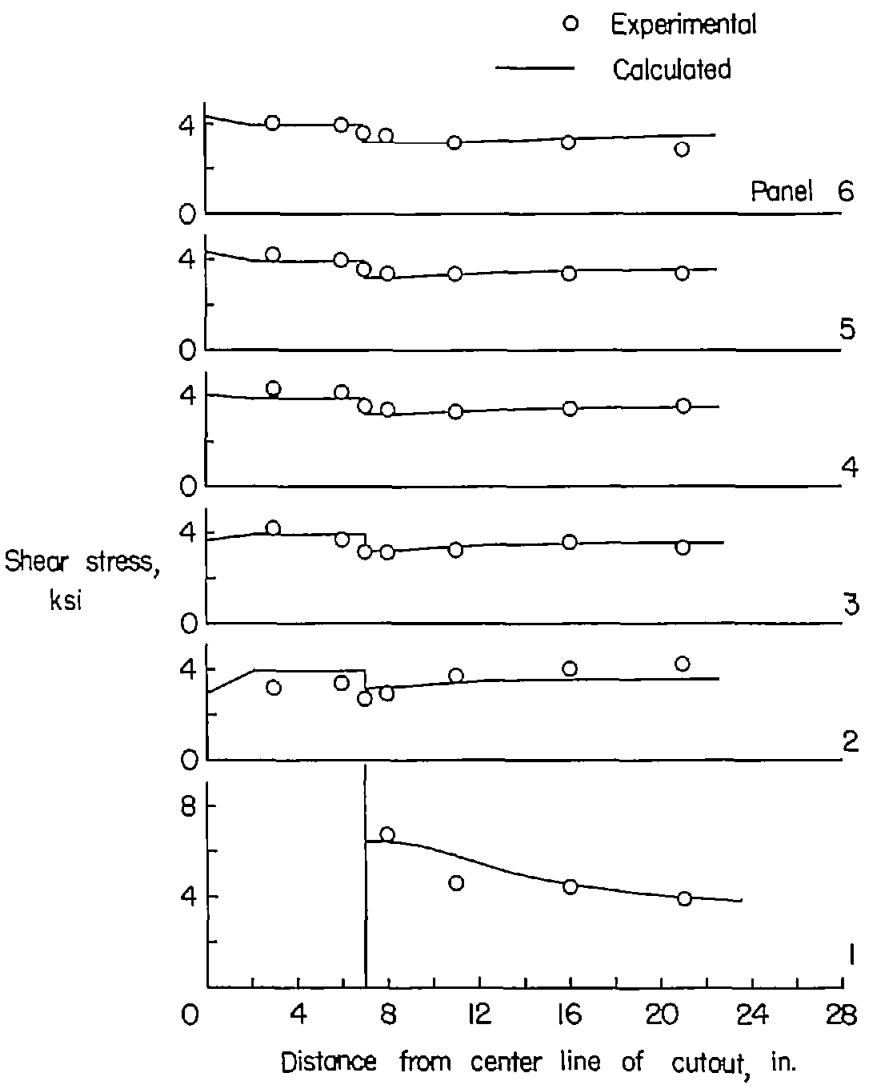

Figure 17.- Shear stresses around cutout one panel wide. Series I; test 4.

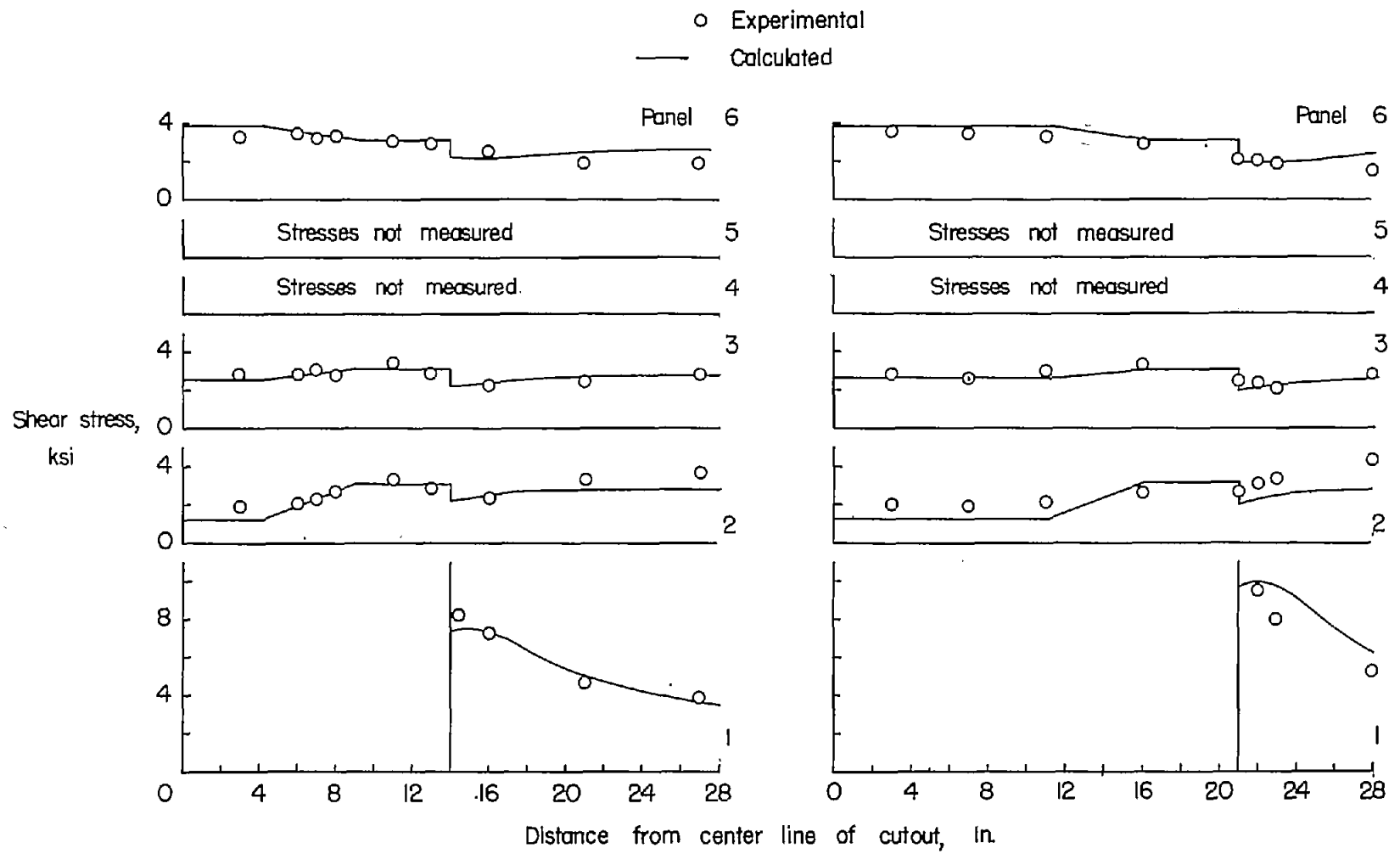

(a) Test 5. (b) Test 6.

Figure 18.- Shear stresses around cutouts one panel wide. Series I.

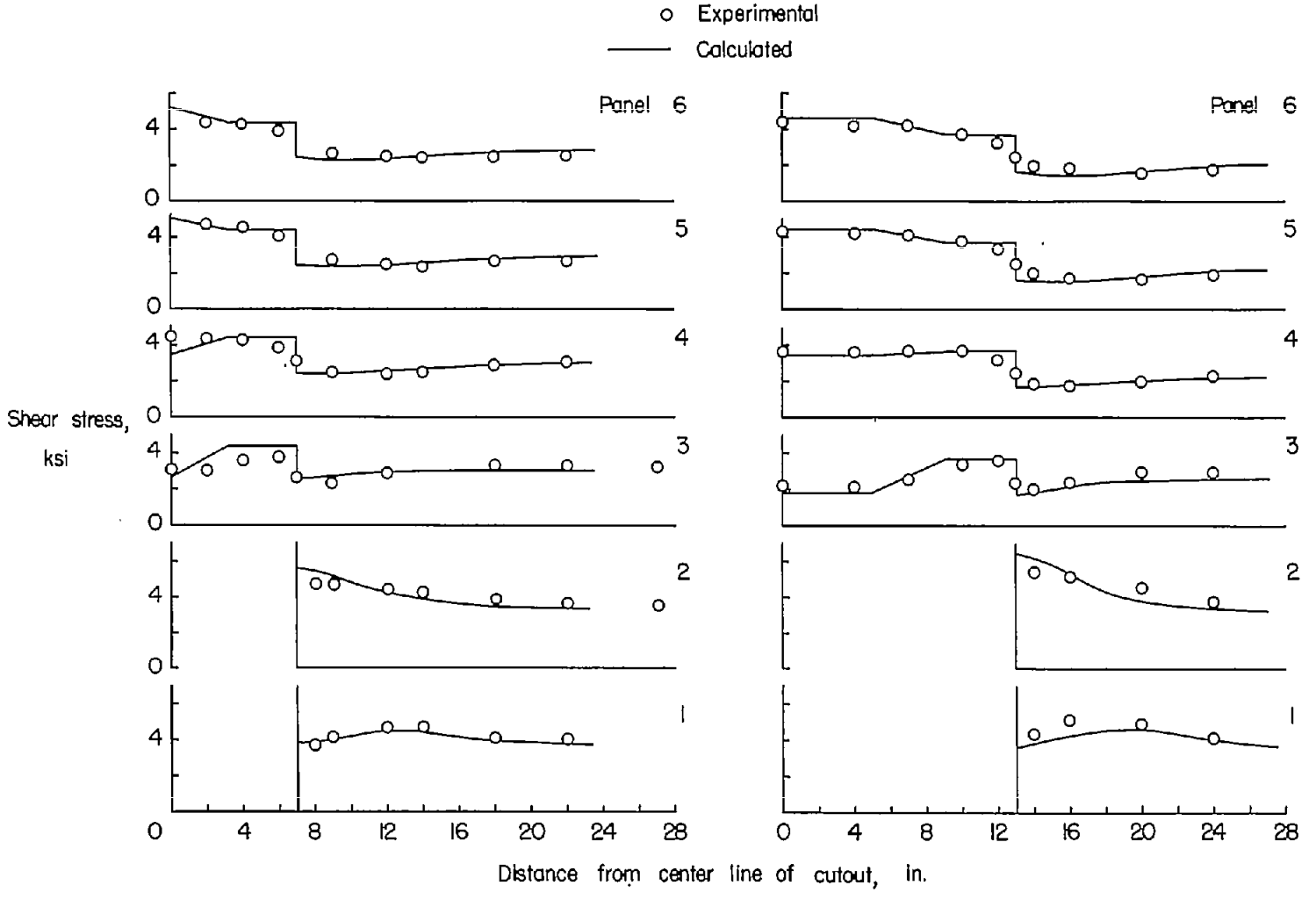

(a) Test 7.

(b) Test 10.

Figure 19.- Shear stresses around cutouts three panels wide. Series I.

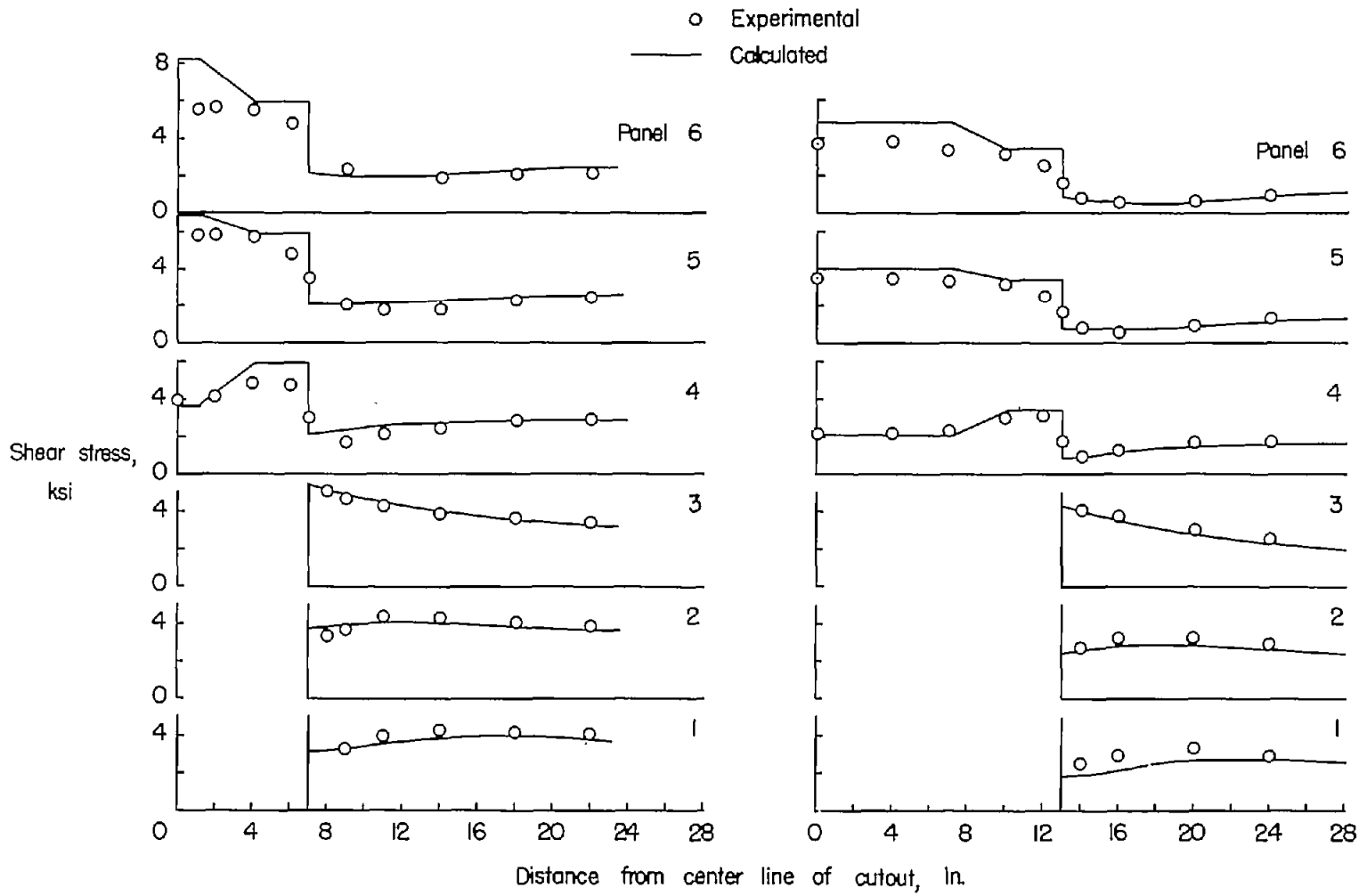

(a) Test 8.

(b) Test 11.

Figure 20.- Shear stresses around cutouts five panels wide. Series I.

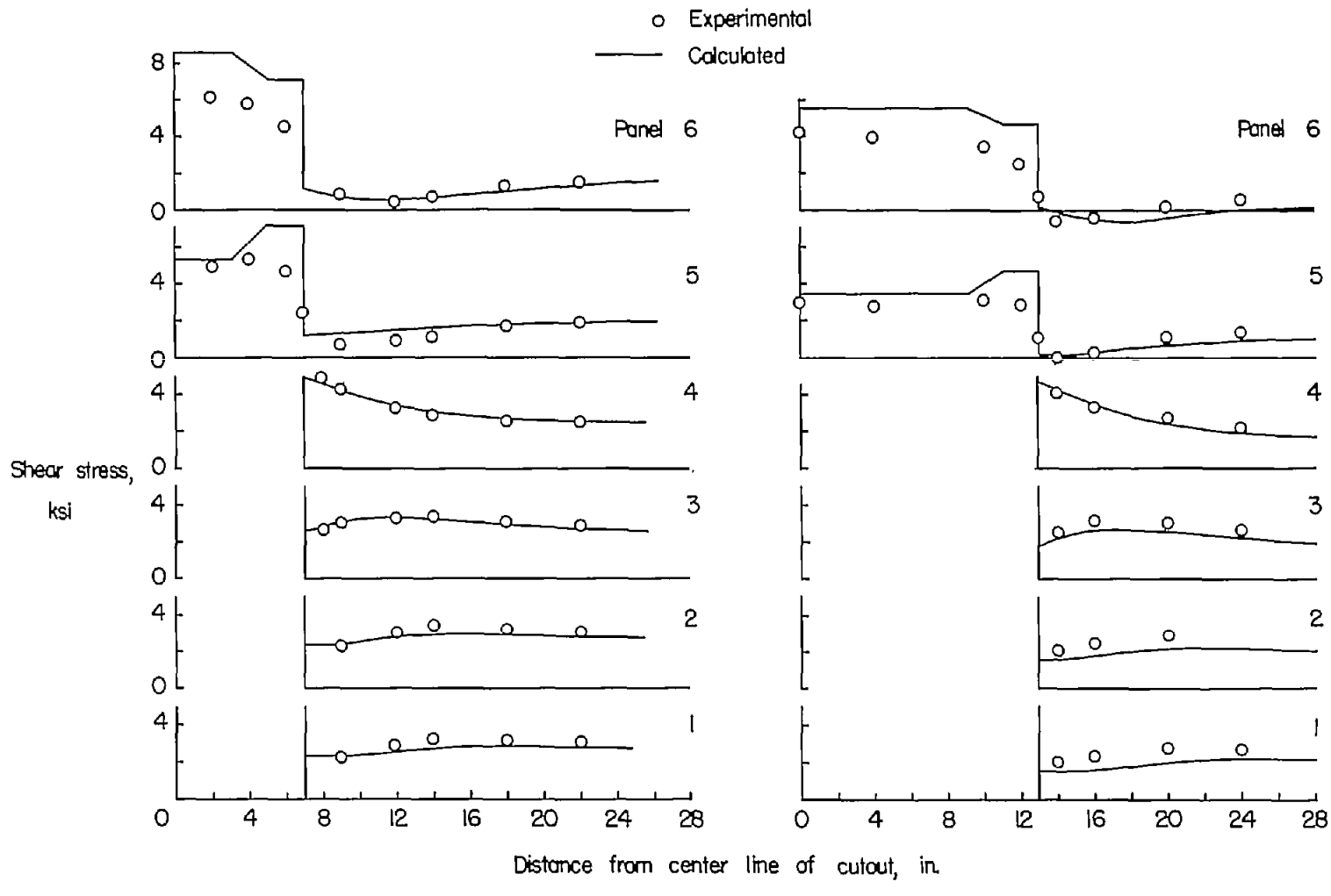

(a) Test 9. (b) Test 12.

Figure 21.- Shear stresses around cutouts seven panels wide. Series I.

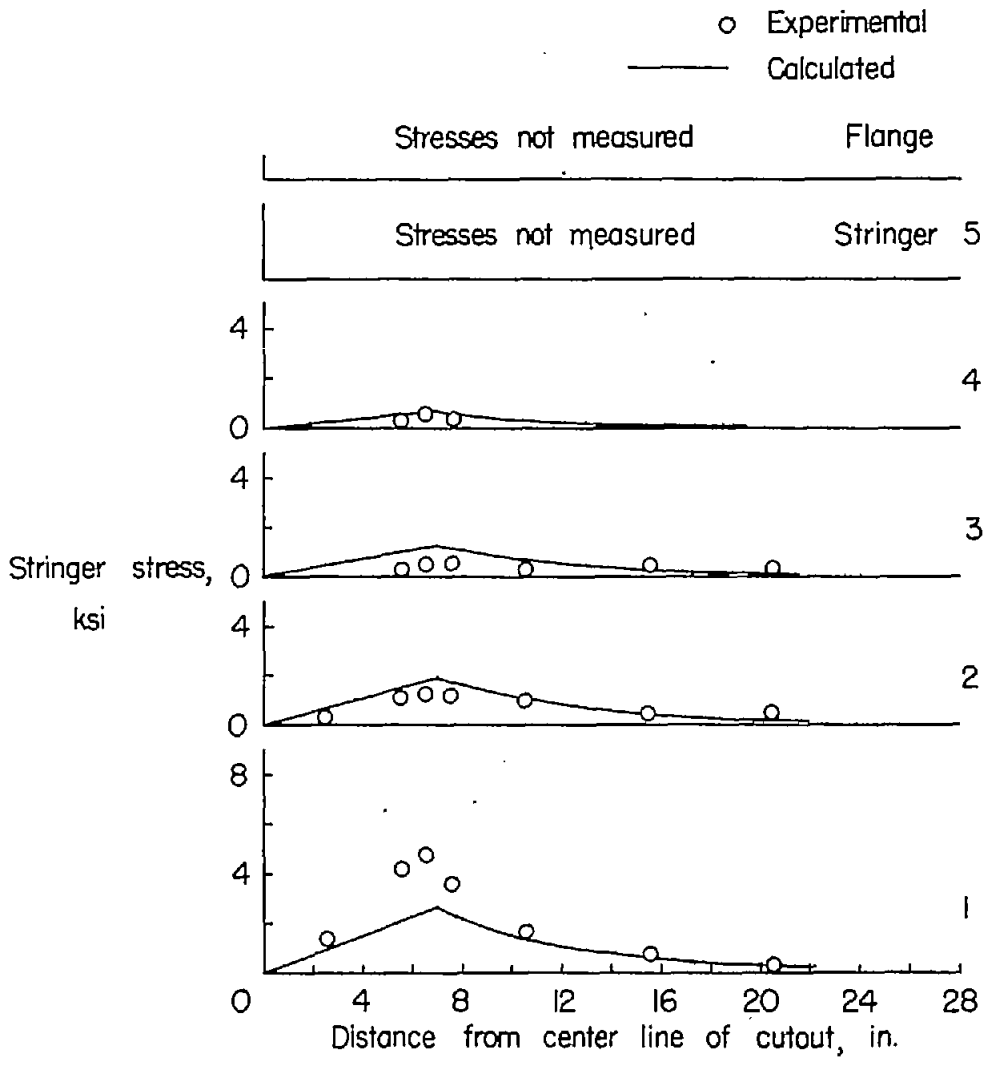

Figure 22.- Stringer stresses around cutout one panel wide. Series I; test 4.

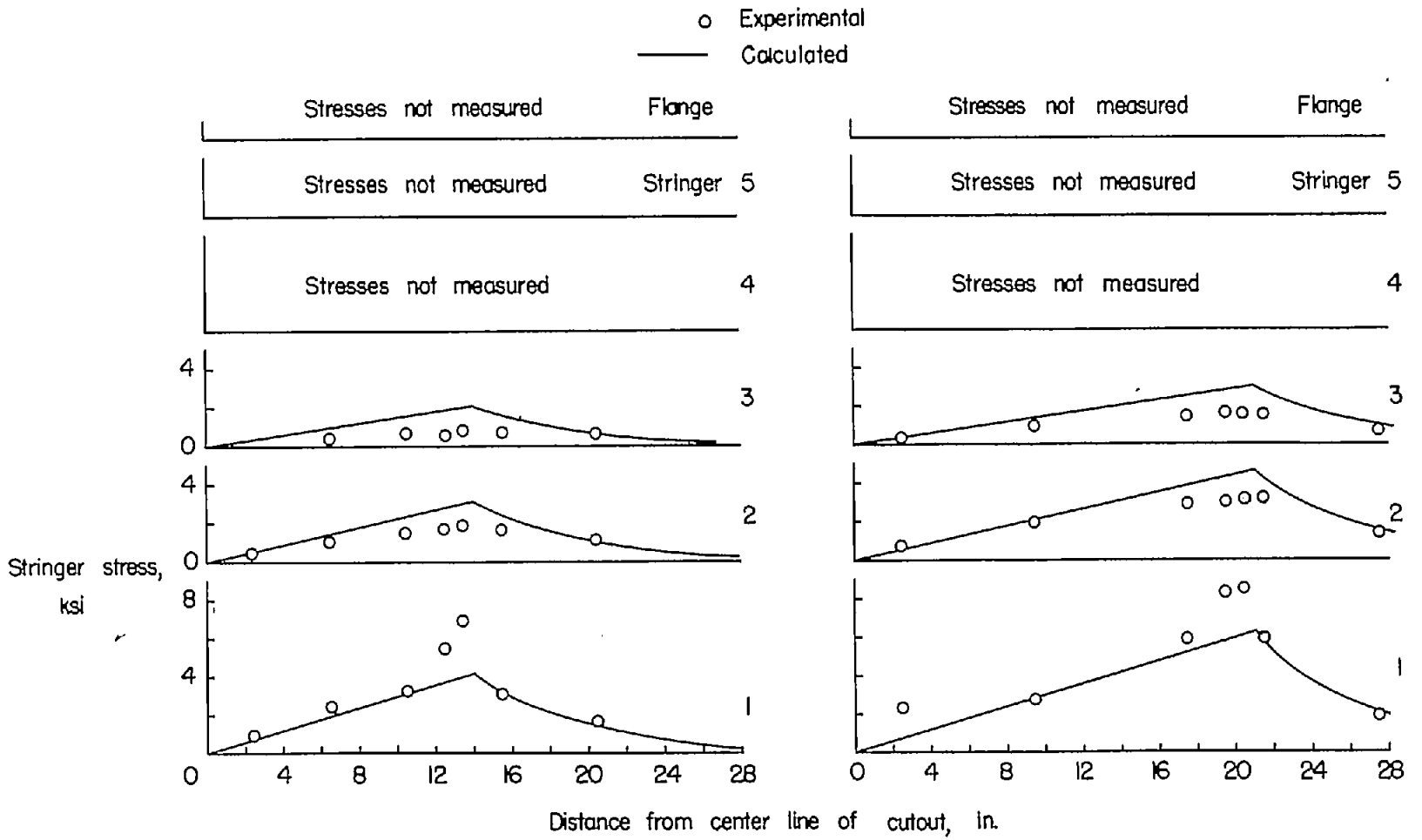

(a) Test 5. (b) Test 6.

Figure 23.- Stringer stresses around cutouts one panel wide. Series I.

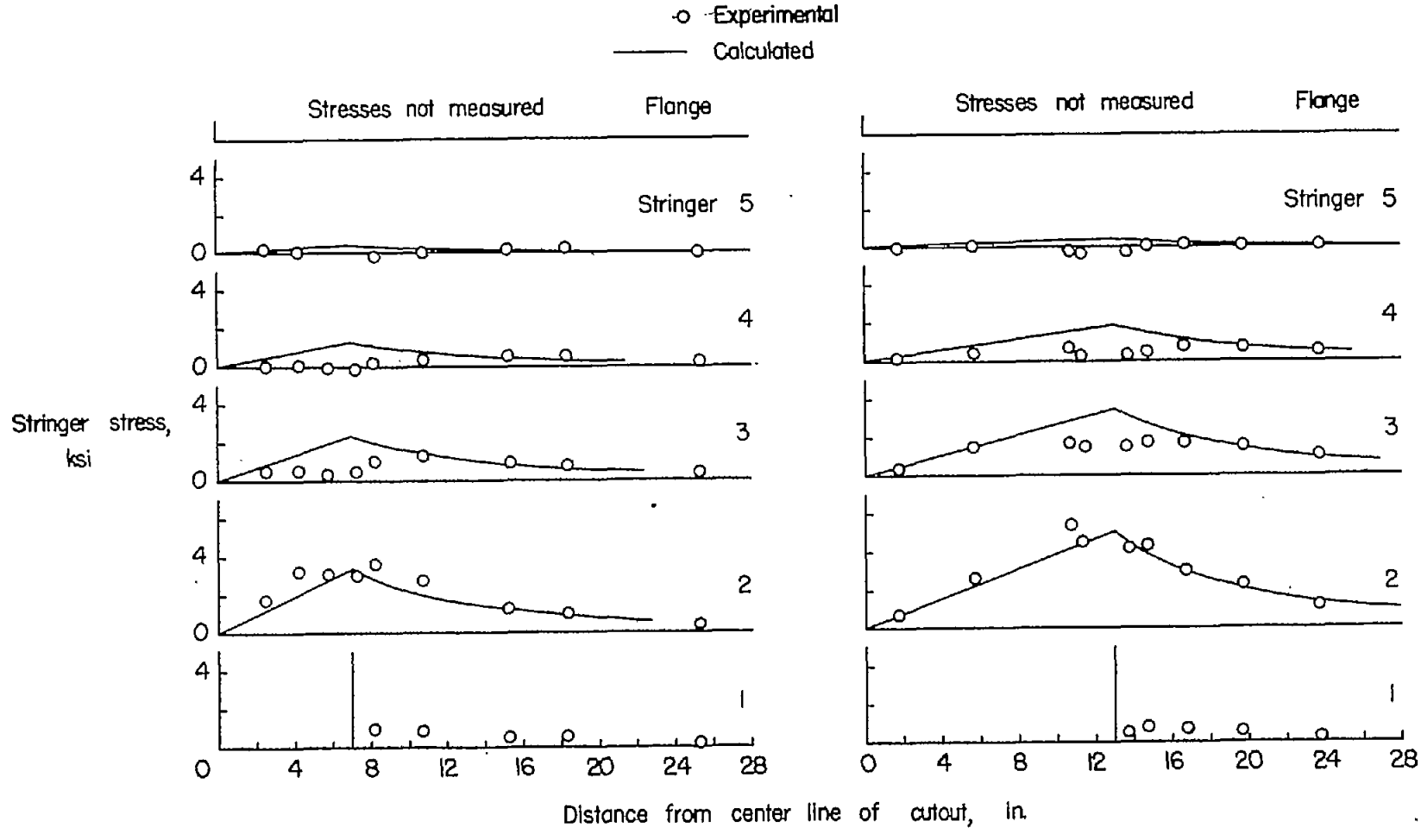

(a) Test 7.

(b) Test 10.

Figure 24.- Stringer stresses around cutouts three panels wide. Series I.

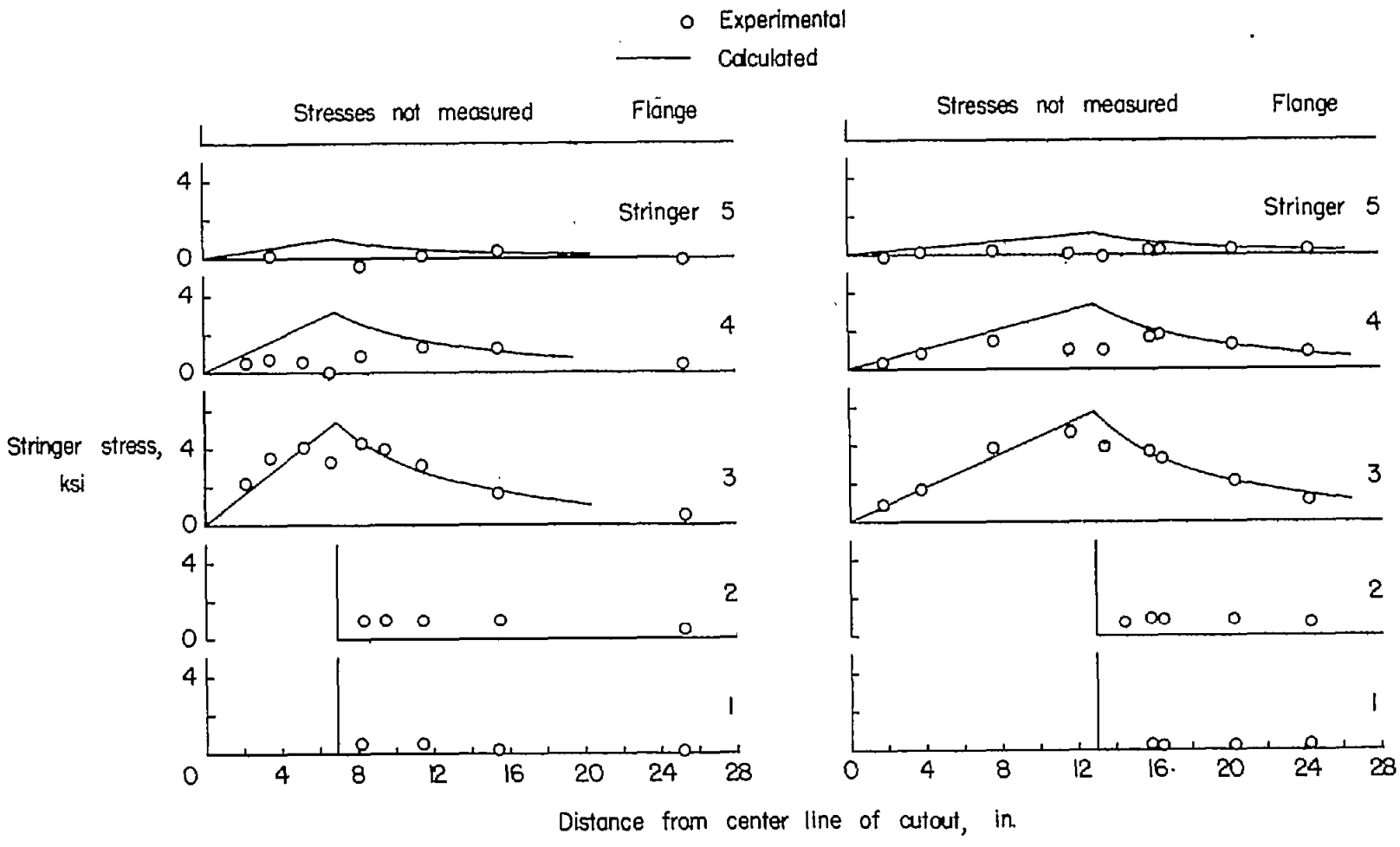

(a) Test 8. (b) Test 11.

Figure 25.- Stringer stresses around cutouts five panels wide. Series I.

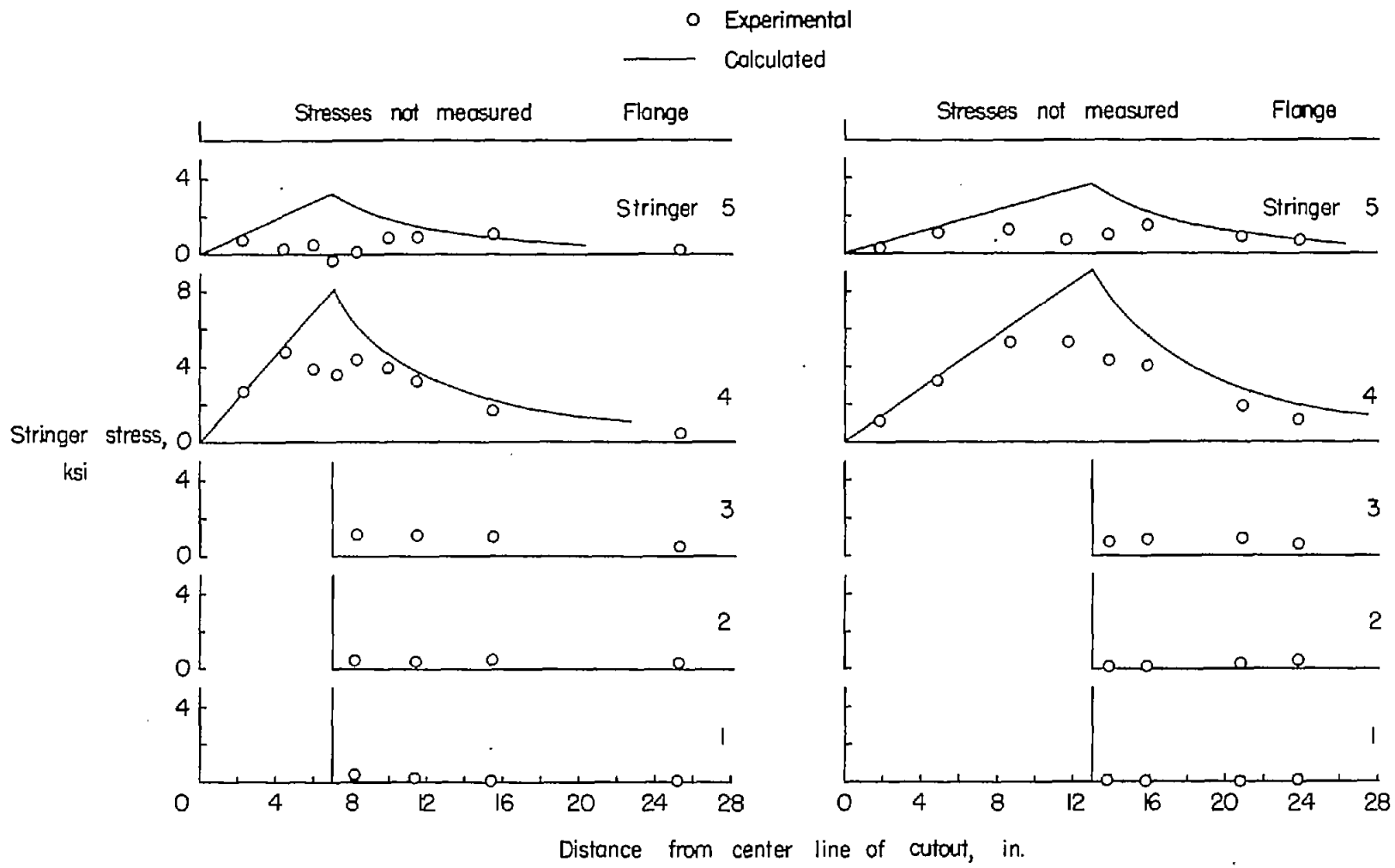

(a) Test 9. (b) Test 12.

Figure 26.- Stringer stresses around cutouts seven panels wide. Series I.

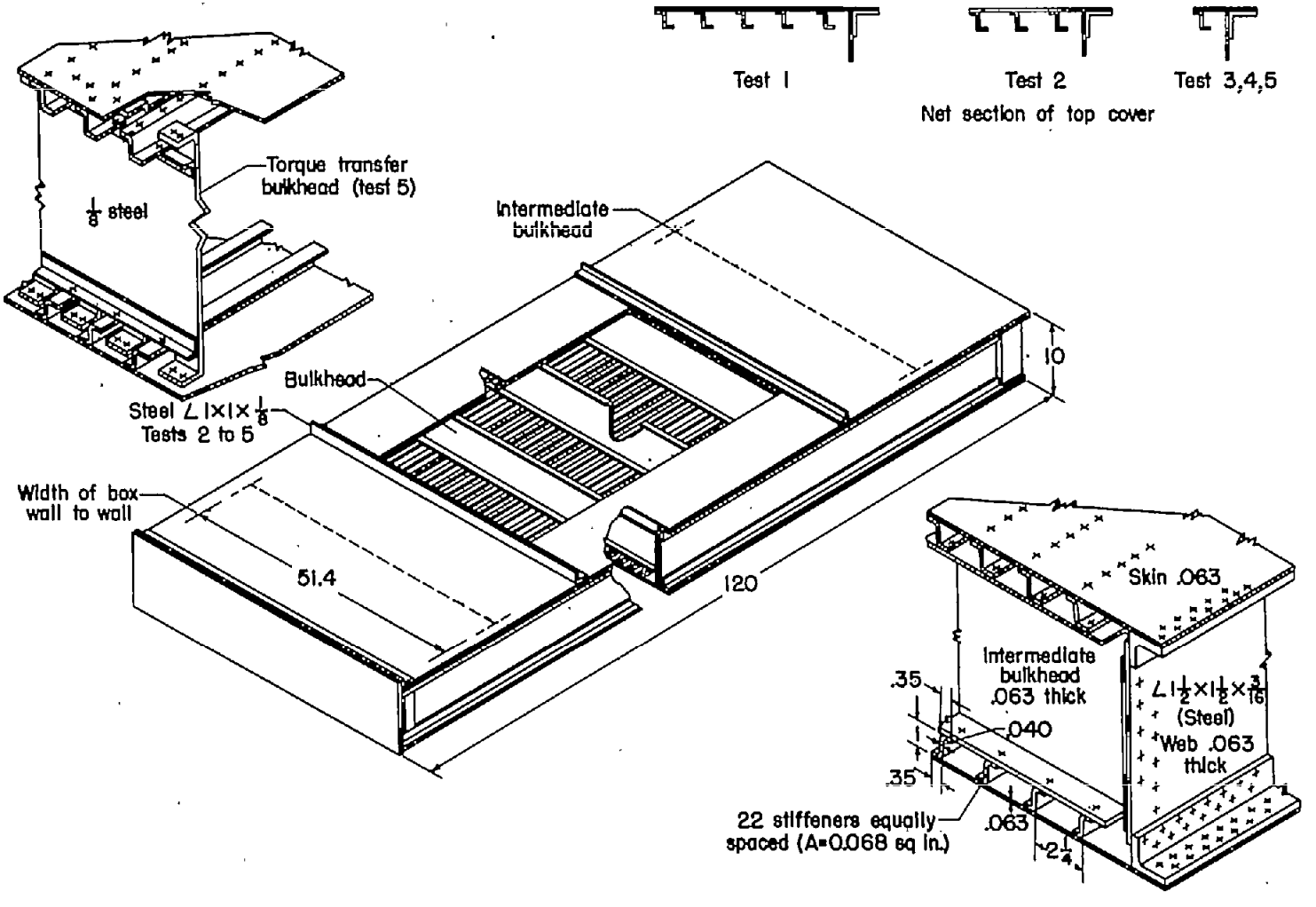

Figure 27.- Test box for series II tests. (All material 24S-T aluminum alloy except where noted.)

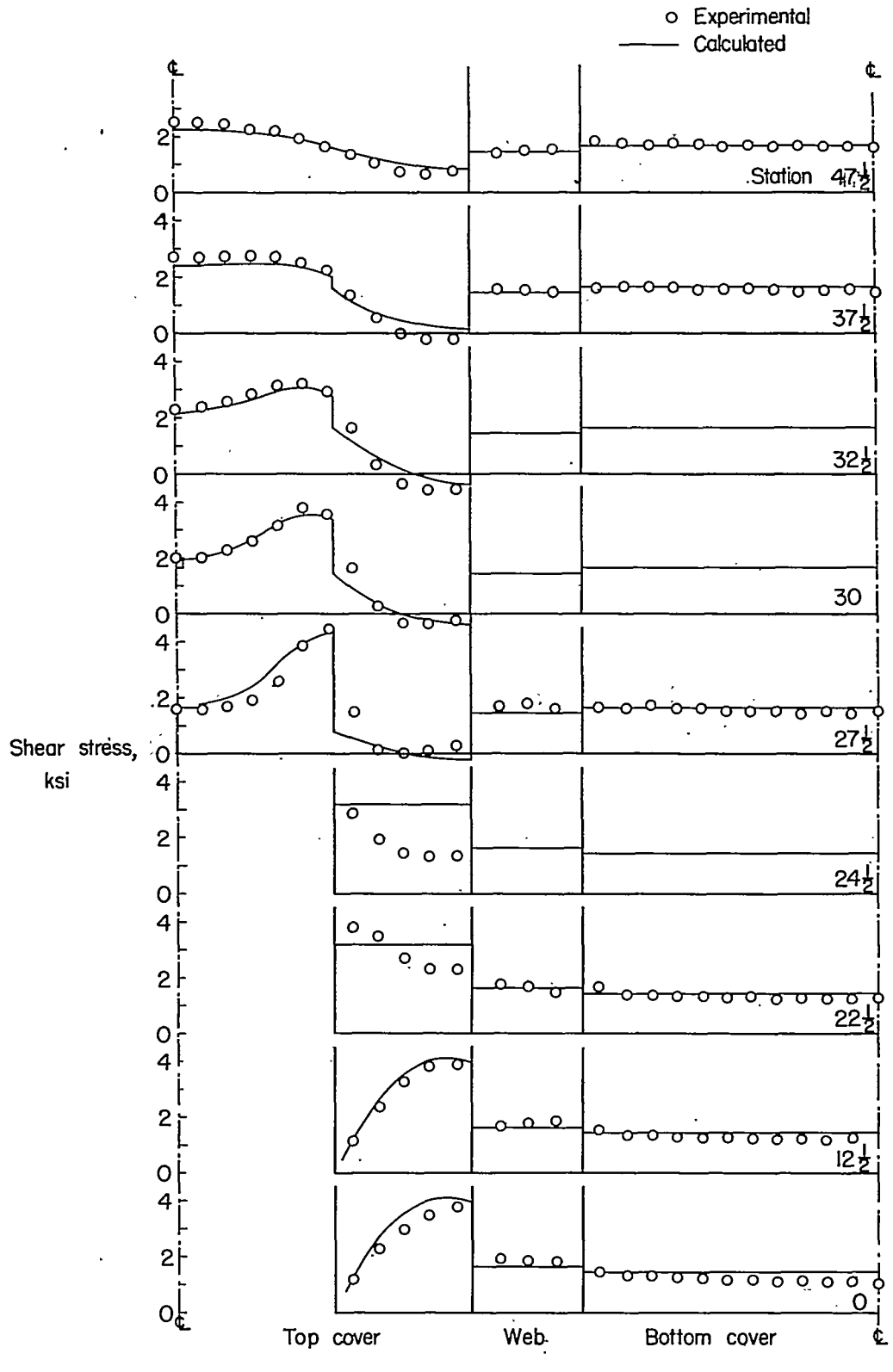

Figure 28.- Shear stresses. Series II; test 1.

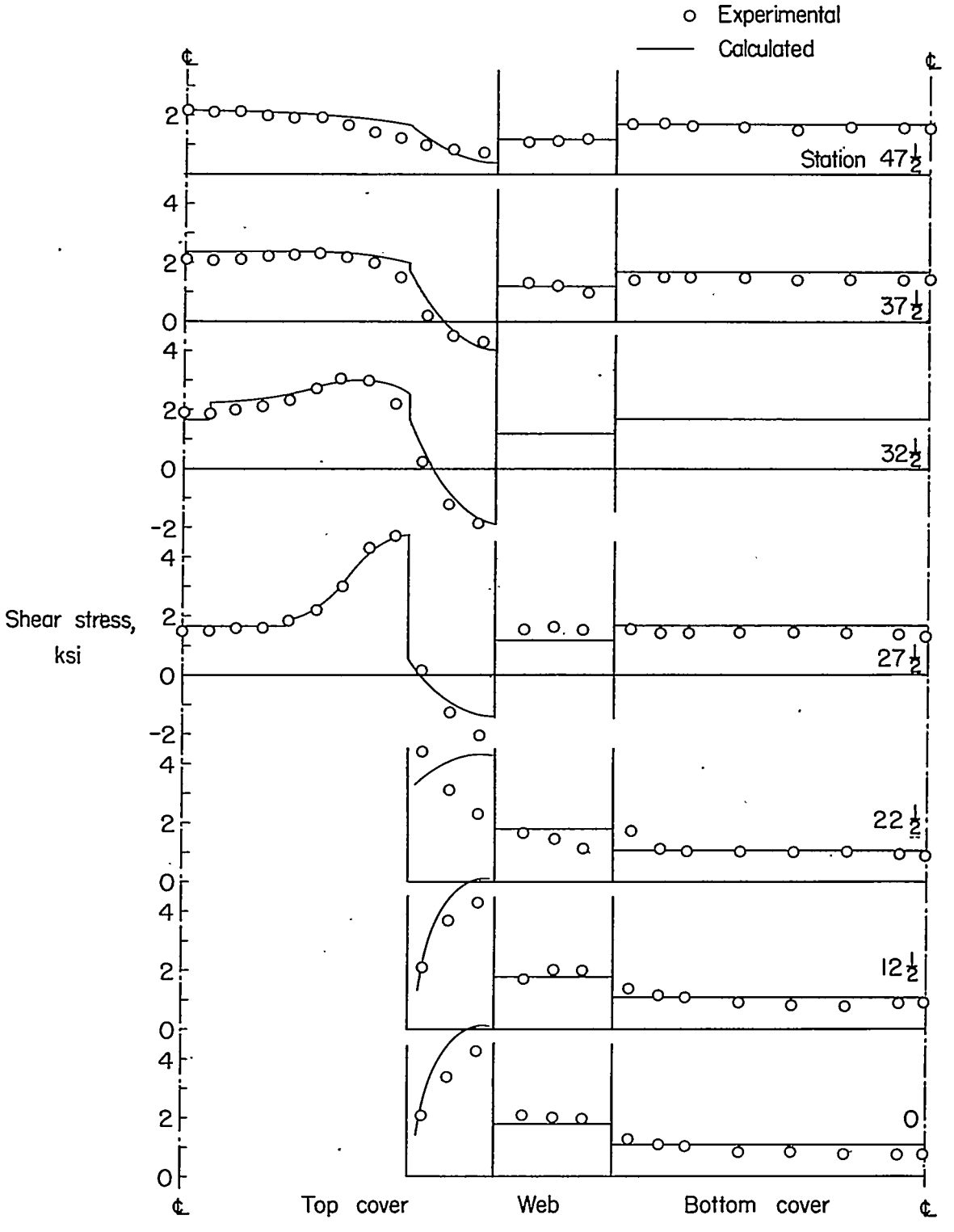

Figure 29.- Shear stresses. Series II; test 2.

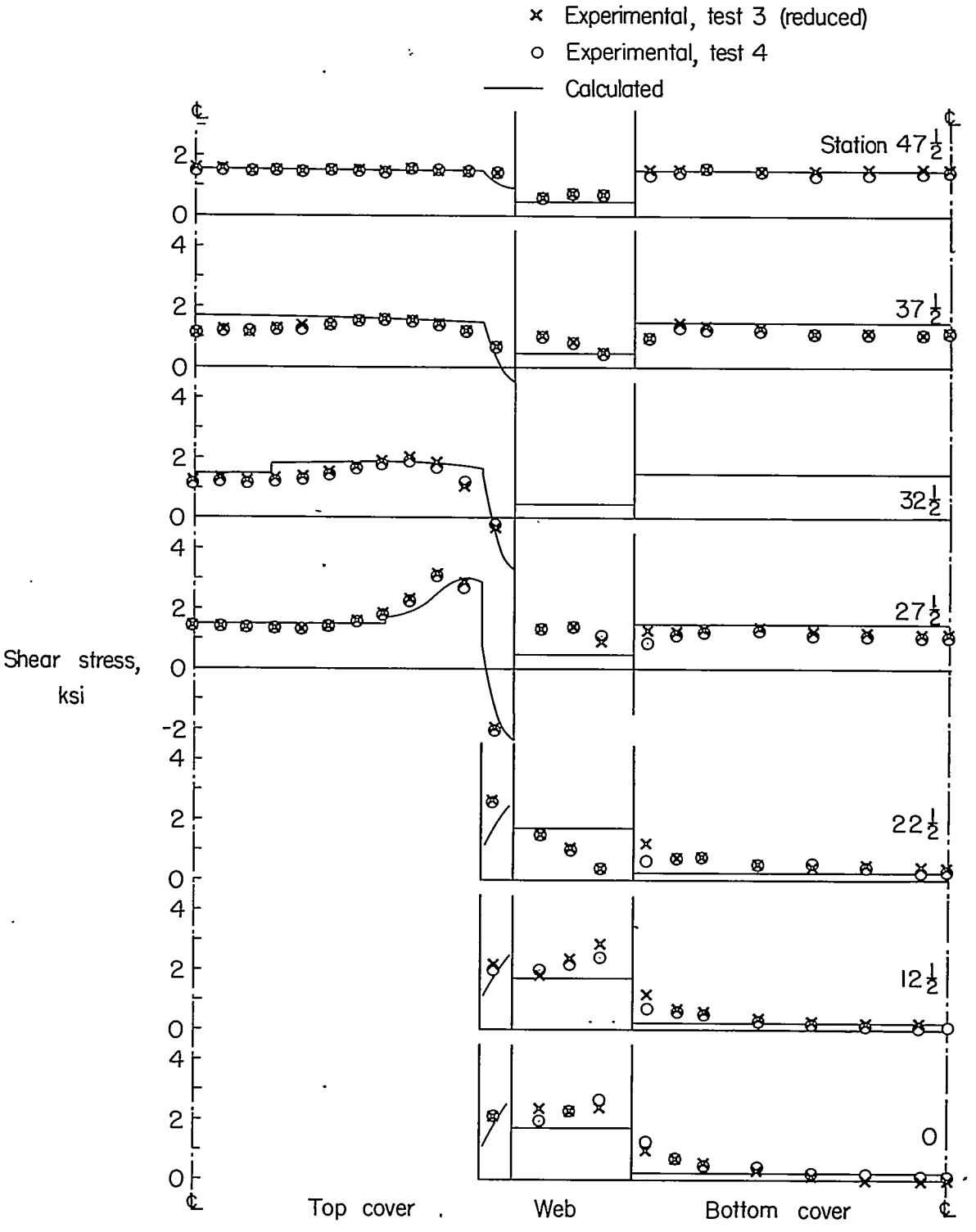

Figure 30.- Shear stresses. Series II; tests 3 and 4.

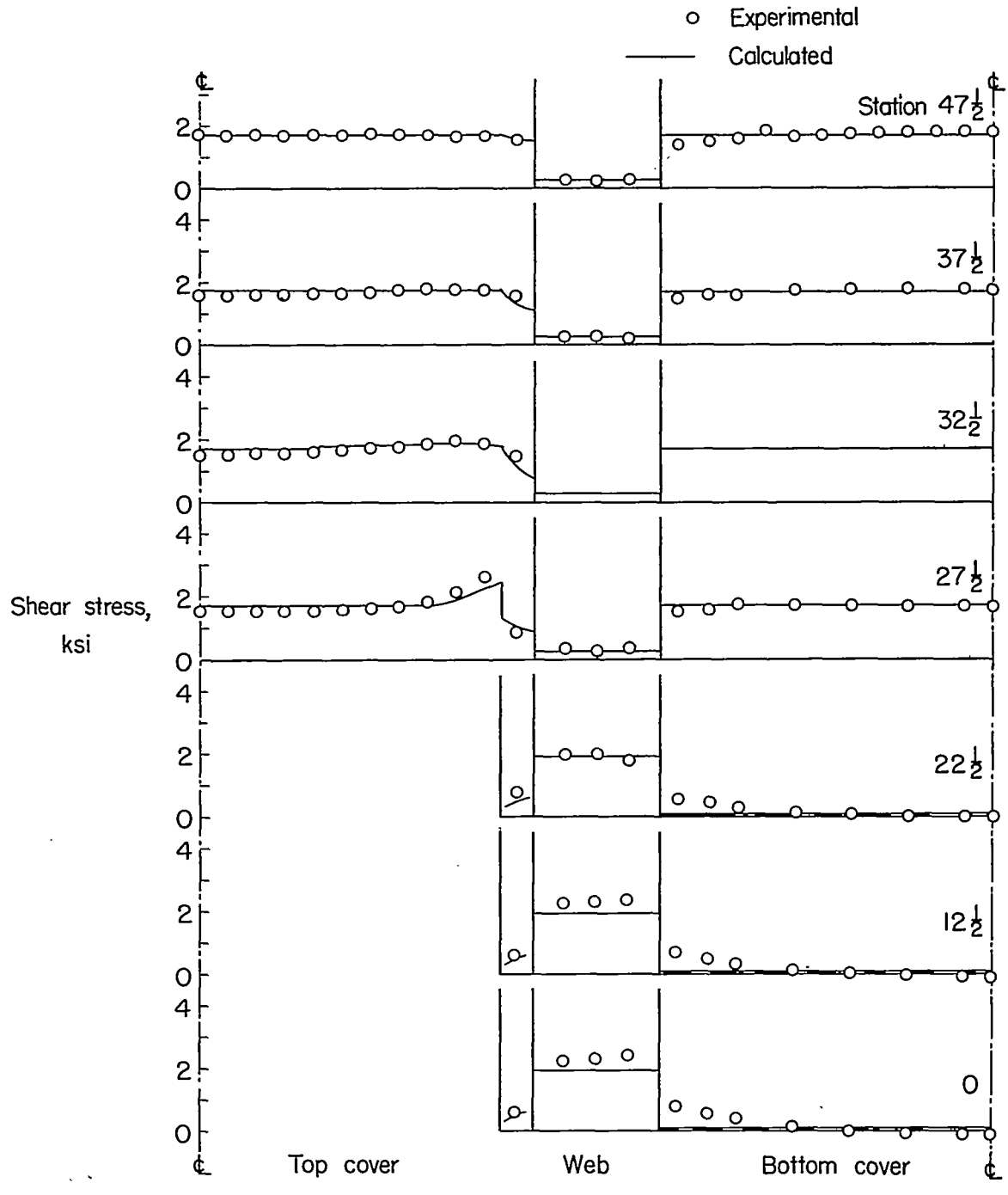

Figure 31.- Shear stresses. Series II; test 5.

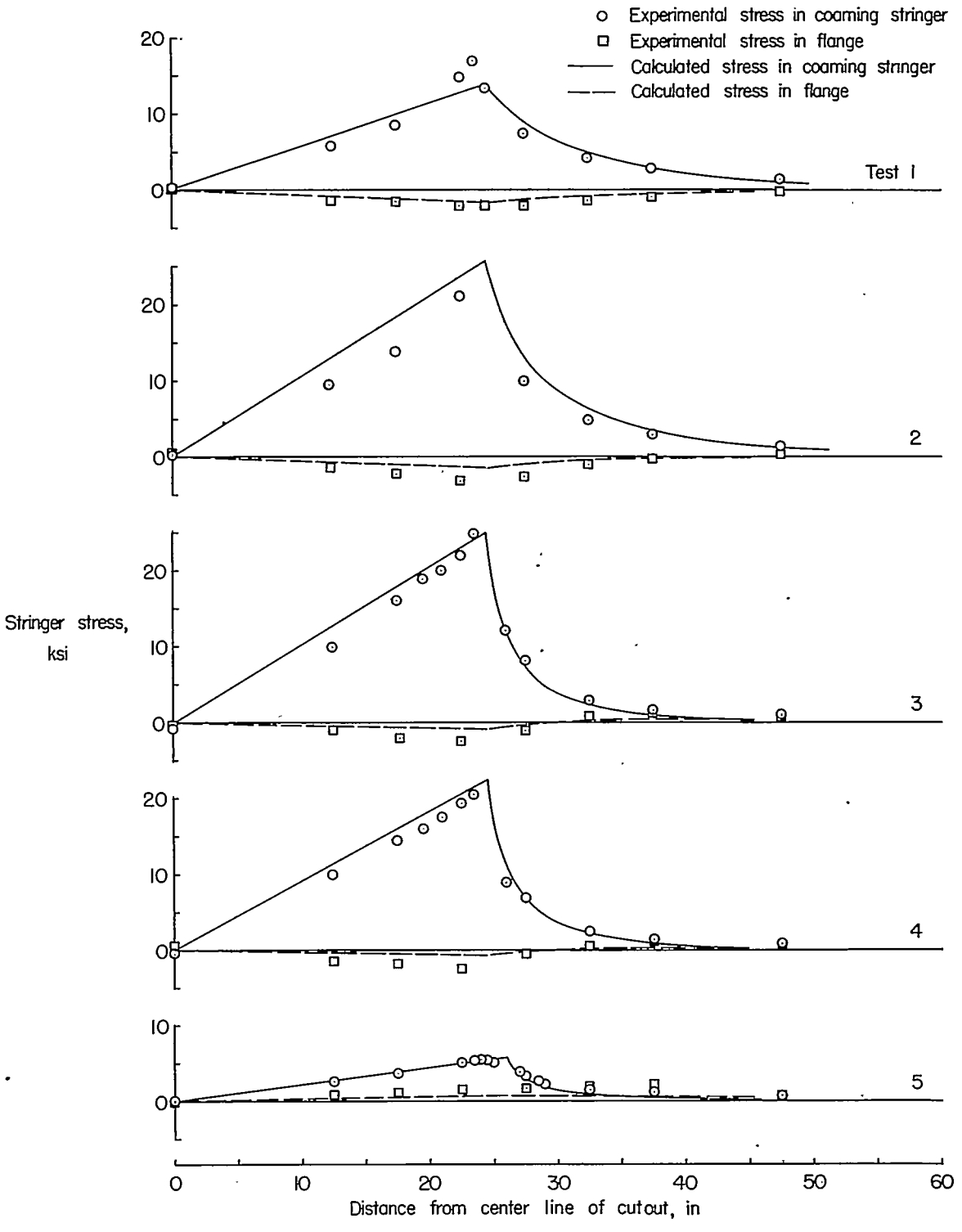

Figure 32.- Stringer stresses. Series II.

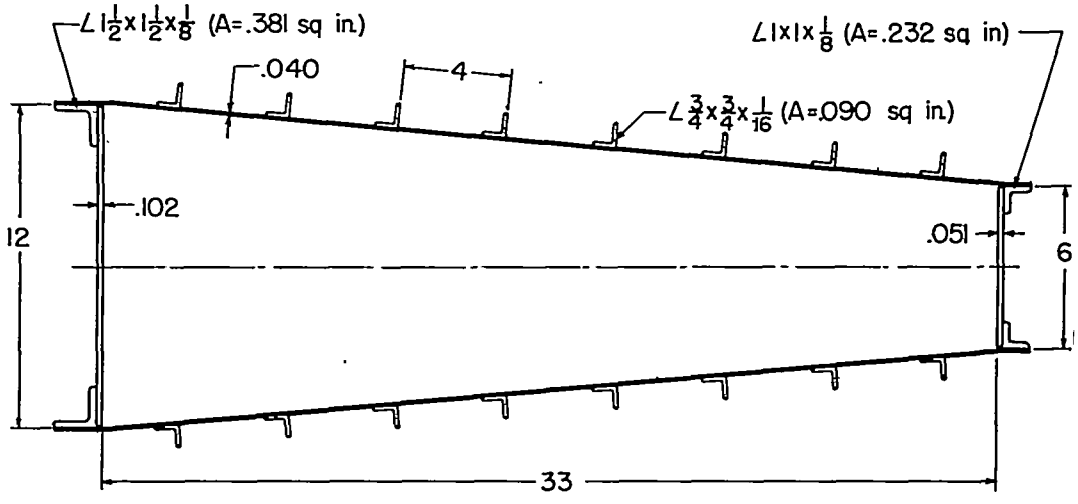

(a) Cross section of test box.

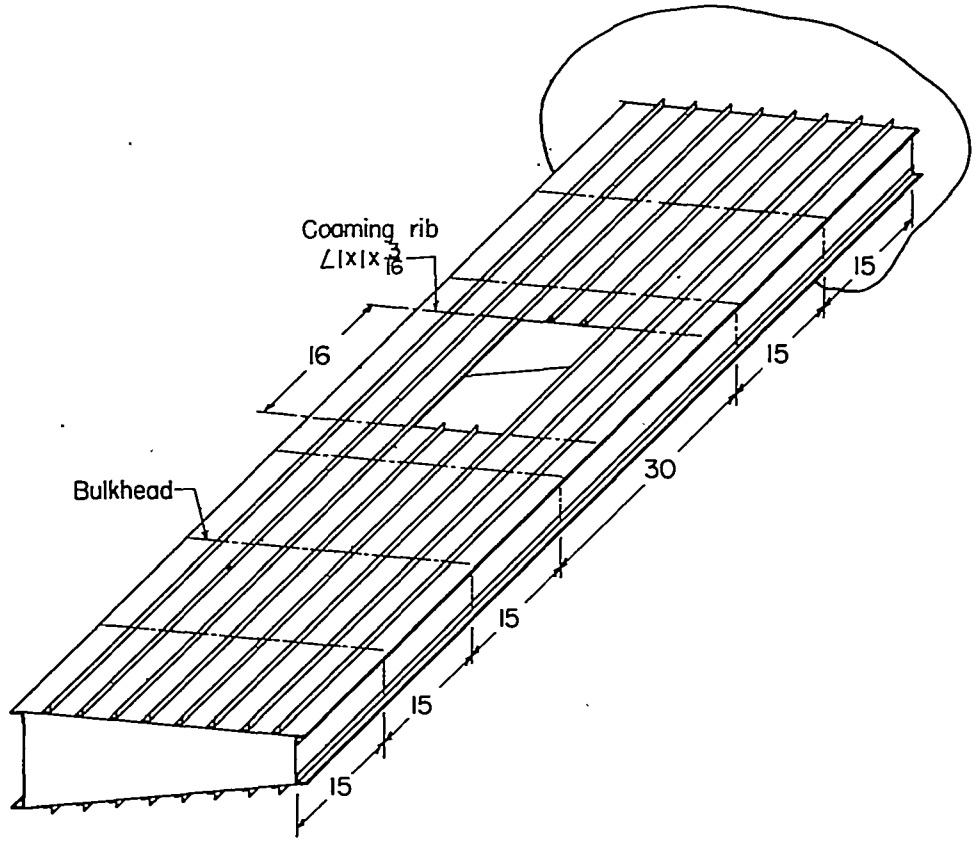

(b) Schematic view of test box.

Figure 33.- Test box for series III tests. (All material 24S-T aluminum alloy.)

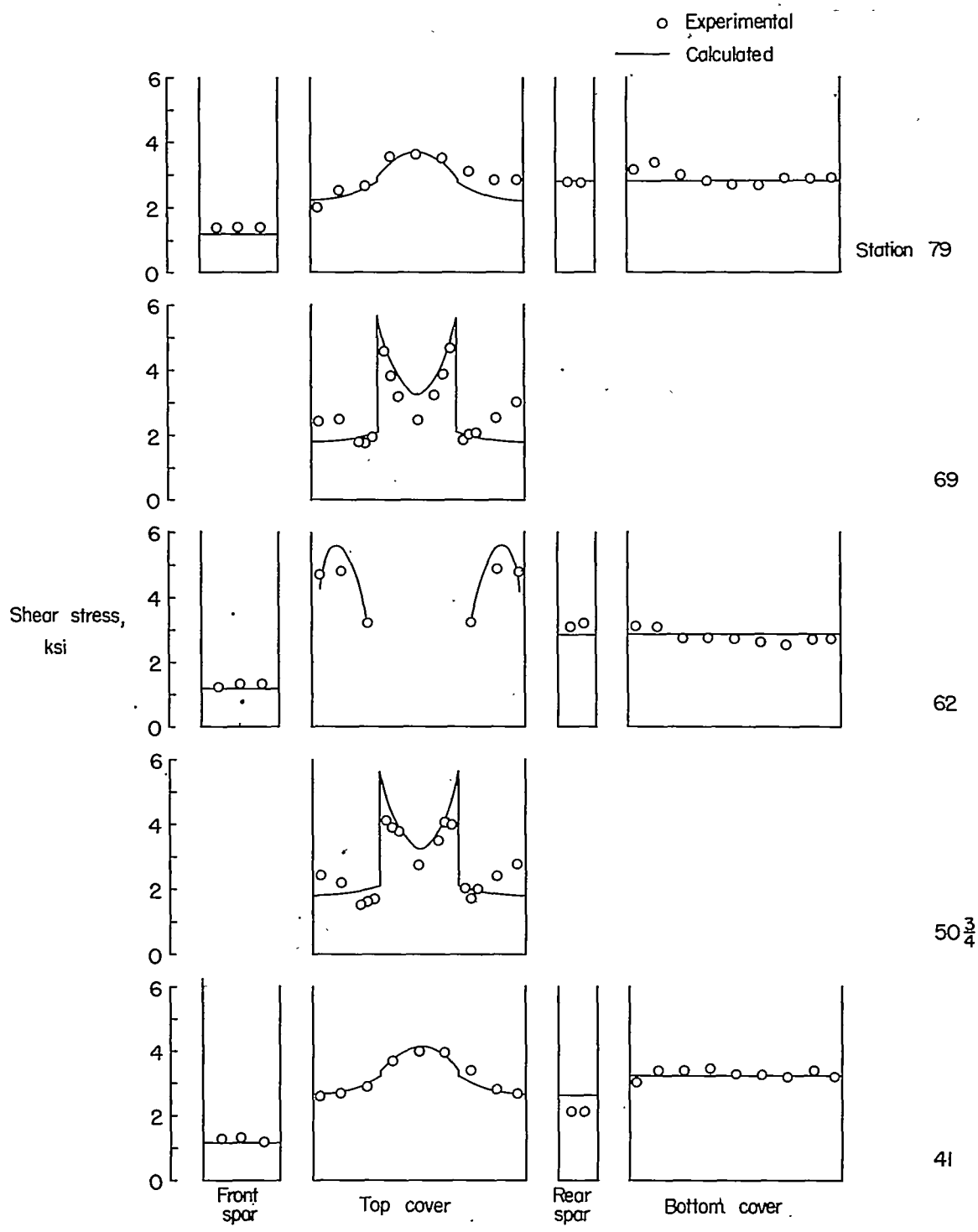

Figure 34.- Shear stresses. Series III; test 1.

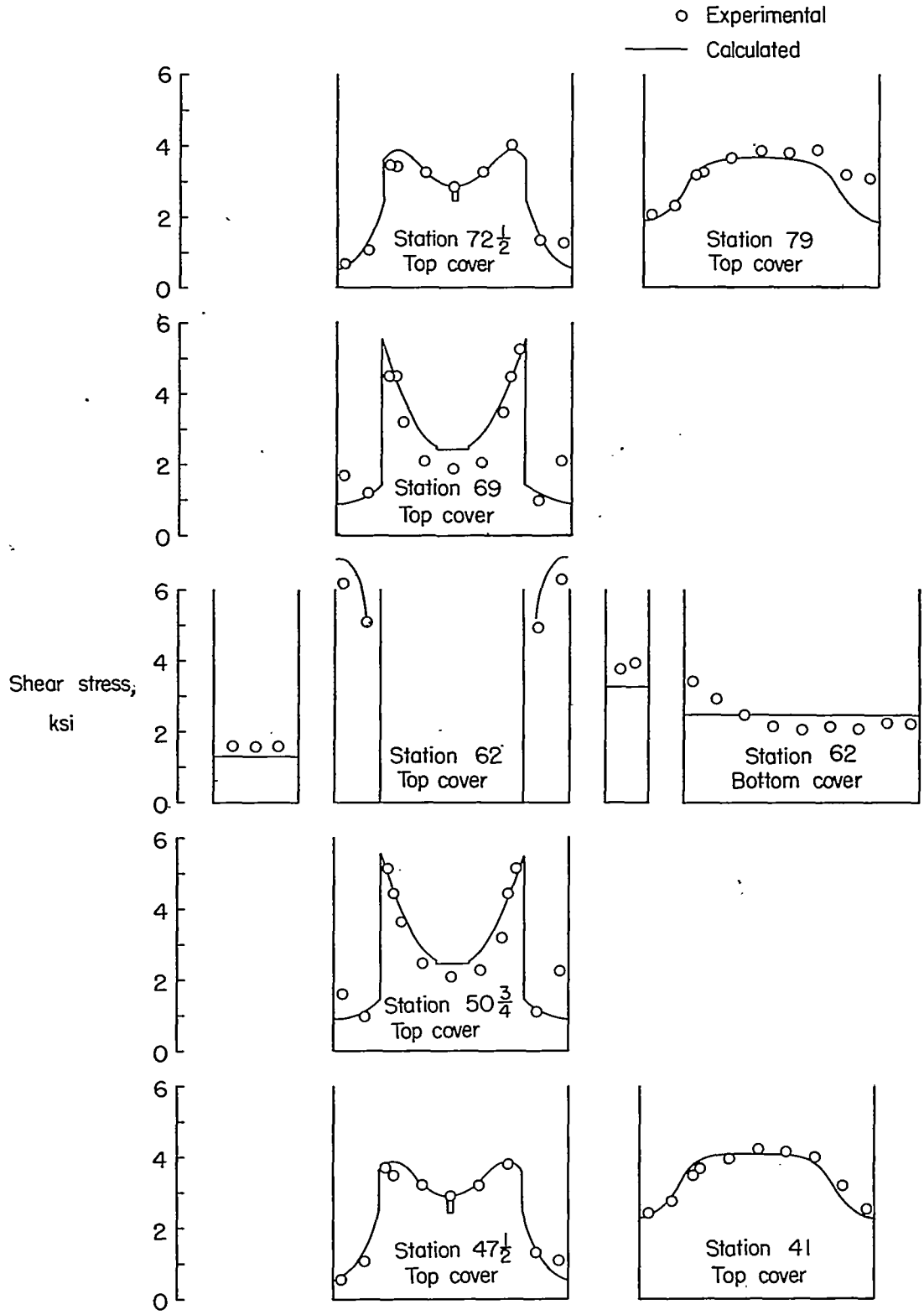

Figure 35.- Shear stresses. Series III; test 2.

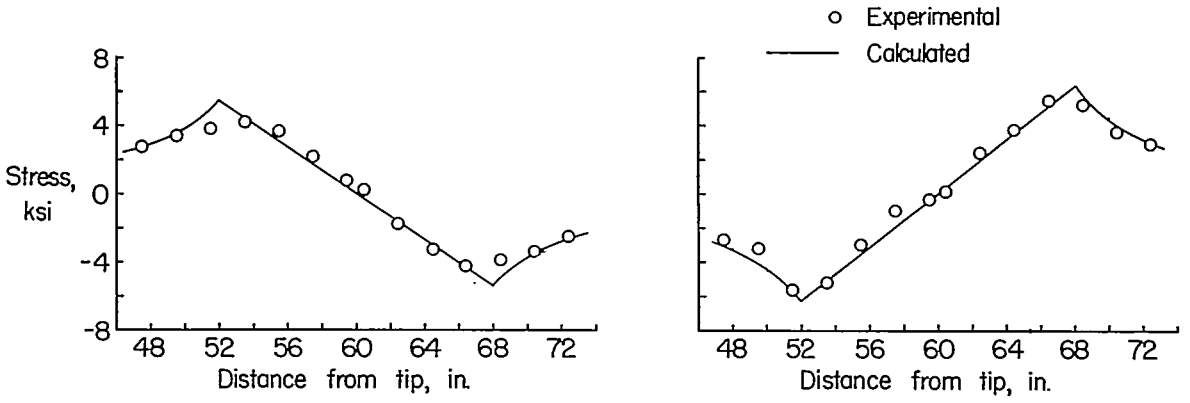

(a) Coaming stringer near front spar. (b) Coaming stringer near rear spar.

Figure 36.- Coaming stringer stresses. Series III; test 1.

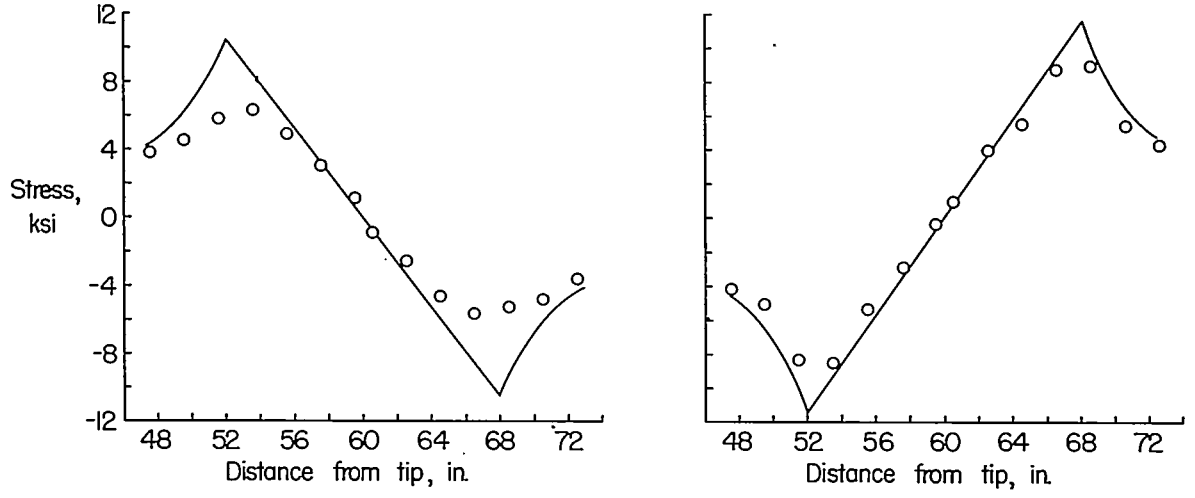

(a) Coaming stringer near front spar. (b) Coaming stringer near rear spar.

Figure 37.- Coaming stringer stresses. Series III; test 2.

NACA-Langley - 12-21-53 - 1000